BMC Chemistry

RESEARCH

Open Access

Synthesis and anticancer evaluation of diaryl pyrido[2,3-*d*]pyrimidine /alkyl substituted pyrido[2,3-*d*]pyrimidine derivatives as thymidylate synthase inhibitors

Adarsh Kumar[1], Nabeel Backer[1†], Harshali Paliwal[1†], Ankit Kumar Singh[1], Tanushree Debbaraman[2], Vikramjeet Singh[3] and Pradeep Kumar[1*]

Abstract

Worldwide, colorectal cancer (CRC) is the third most common type of cancer and the second most common cause of cancer-related deaths. Thymidylate synthase (TS) is a crucial component of DNA biosynthesis and has drawn interest as an essential target for cancer treatment. In the current work, we have designed and synthesized twenty-eight new diaryl-based pyrido[2,3-*d*]pyrimidine/alkyl-substituted pyrido[2,3-*d*]pyrimidine derivatives and evaluated their anticancer activity against the HCT 116, MCF-7, Hep G2, and PC-3 cell lines cell lines. Additionally, we have carried out TS inhibitory activity and *in silico* studies for compounds 1n and 2j. All the synthesized compounds exhibited good anticancer activity, but among them, compounds 1n and 2j showed excellent anticancer activity, having IC_{50} values of 1.98 ± 0.69, 2.18 ± 0.93, 4.04 ± 1.06, and 4.18 ± 1.87 µM; and 1.48 ± 0.86, 3.18 ± 0.79, 3.44 ± 1.51, and 5.18 ± 1.85 µM, against the HCT 116, MCF-7, Hep G2, and PC-3 cell lines respectively with control raltitrexed (IC_{50} 1.07 ± 1.08, 1.98 ± 0.72, 1.34 ± 1.0, and 3.09 ± 0.96 µM, respectively) and hTS inhibitory activity with IC_{50} values of 20.47 ± 1.09 and 13.48 ± 0.96 nM with control raltitrexed (IC_{50} 14.95 ± 1.01 nM). Further, the mechanism of inhibition was revealed by molecular docking, which showed the binding pattern of 1n and 2j to the catalytic site of TS with docking scores of -10.6 and −9.5 kcal/mol, respectively, with reference raltitrexed (-9.4 kcal/mol). Additionally, the assessment of physicochemical, biochemical, structural, and toxicological characteristics were also in the acceptable range for these compounds. Based on the anticancer activity of compounds, SAR was also performed for lead optimization.

Keywords Colorectal cancer, Pyrido[2,3-*d*]pyrimidine, Thymidylate synthase, Anticancer, In silico studies

†Nabeel Backer and Harshali Paliwal may be treated as second author.

*Correspondence:
Pradeep Kumar
pradeepyadav27@gmail.com
[1]Department of Pharmaceutical Sciences and Natural Products, Central University of Punjab, Bathinda 151401, India
[2]Rajiv Gandhi Centre for Diabetes & Endocrinology, J N Medical College & Hospital, Aligarh Muslim University, Aligarh 202002, UP, India
[3]Department of Pharmaceutical Sciences, Guru Jambheshwar University of Science and Technology, Hisar 125001, HR, India

Introduction

Numerous people around the world are impacted by cancer, which is a significant health concern [1–3]. Globally, colorectal cancer (CRC) is the second most common cause of cancer-related mortality and the third most common cancer [4]. According to the Globocan report, 2022, 19,964,811 new cases of cancer have been reported throughout the world; among them, 1,926,118 (9.6%) were colorectal cancer cases and 904,000 colorectal cancer deaths. This amounts to nearly one in ten cancer-related deaths and cases [5]. Elderly patients are typically diagnosed with CRC. The median age of CRC diagnosis in the USA was 67 years from 2013 to 2017, while 68% of new cases are anticipated to occur in people over 65 during 2020. The American Cancer Society estimated 106,970 new cases of colon cancer and 46,050 new cases of rectal cancer in the United States for 2023 [6].

Human thymidylate synthase (hTS) is gaining attention in cancer chemotherapy because of its crucial function in DNA biosynthesis [7]. It is a rate-limiting enzyme in the *de novo* production of 2-deoxythymidine-5-monophosphate, which is required for DNA synthesis [4]. Nitrogen-containing heterocyclic compounds, such as β-lactam, quinoxaline, pyrazole, pyrrolobenzodiazepine, pyrido[2,3-*d*]pyrimidines, quinoline, quinazoline, pyrimidine, benzimidazole, pyridine, carbazole, imidazole, triazole, indole, and isatin, are widely recognized pharmacophores in medicinal chemistry, exhibiting a variety of pharmacological actions. The effect of pyrido[2,3-d] pyrimidine derivatives on cancer has not received as much attention as those of the other nitrogen-containing heterocyclic compounds mentioned [8]. Therefore, to explore the role of pyrido[2,3-*d*]pyridine in cancer treatment, we have performed a detailed literature search and found that eleven different cancer targets, including tyrosine kinase, extracellular regulated protein kinases - ABL kinase, etc. have been reported worldwide, but not a single molecule explored on TS [1].

Therefore, we have designed and synthesized benzylated diaryl-based pyrido[2,3-*d*]pyrimidine /alkyl substituted pyrido[2,3-*d*]pyrimidine derivatives to explore their hTS inhibitory potential. The designed compounds were developed on the basis of reported pyrido[2,3-*d*] pyrimidine derivatives as anticancer agents [1]. The compound considered for the drug design was 2-(2-(4-Fluorobenzylidene)hydrazinyl)-5-phenyl-7-(thiophen-2-yl) pyrido[2,3-d]pyrimidin-4(3 H)-one (I) (Fig. 1), reported by Fares M. *et al.* [9]. The molecules of the present series were designed by replacing thiophene with an aromatic ring and substituting hydrazine with a carbonyl group (as that of 5-FU), as it is a primary requirement of hTS inhibitors. Further, the free NH of reported molecules has also been substituted with methyl (Fig. 1). The designed compounds were docked into the catalytic pocket of hTS (PDB code: 1HVY). The docking score and interactions of designed compound 1n revealed the molecules bind similar to raltitrexed within the active site of hTS, and all the designed compounds had better docking scores than the reported inhibitors (I), 5-FU and raltitrexed (Table 1).

Materials and methods

General chemistry

We used the starting ingredients and solvents purchased from commercial suppliers without further purification. Silica gel 60 F_{254} was used for identification, and TLC was utilized to monitor the reaction's progress. Silica gel 60–120 and solvent ethyl acetate/$CHCl_3$ and petroleum ether were used for column chromatography. A 600 MHz Jeol NMR spectrometer was used to record ^{1}H NMR and ^{13}C NMR spectra in $CDCl_3/d_6$-DMSO, with TMS ($\delta=0$) as the internal standard. The splitting patterns are singlet (s), doublet (d), triplet (t), and multiplet (m), and the chemical shifts are reported in δ ppm. The coupling constant values are expressed in hertz (Hz). Uncorrected melting points were determined using an open glass capillary tube and a Stuart melting point instrument (SMP-30). GCMS spectra were recorded by SHIMADZU GCMS at 70 eV. UV Visualization of TLC was done by Spectroline Fluorescence Analysis Cabinet (Model CM-10 A). FTIR of synthesized molecules was recorded by FTIR 4X (Make-JASCO). HRMS spectrum of lead inhibitors 1n and 2j was recorded by Triple TOF 5600 (Make-SCIEX). HPLC of potent compounds was performed on Agilent 1260 Infinity II with column Eclipse XDB-C18, having a particle size of 5 µm.

Synthetic procedure and spectral data

General procedure for the synthesis of intermediate (I)

A round bottom flask charged with 100 ml of pure methanol containing 6.011 g of sodium ethoxide (1 eq.) was used to dissolve 10 gm of cyanoacetic ester (1 eq). After that, urea (1 eq) was added, and the mixture was heated over reflux for 10 h. The alcohol was subsequently removed, and the remaining substance was dissolved in water. By adding acetic acid, the 6-aminopyrimidine-2,4(1 *H*,3 *H*)-dione precipitated out, which was collected by filtering [10].

General procedure for the synthesis of substituted chalcone (II)

In a 100 ml round bottom flask, substituted benzaldehyde (1 eq) was dissolved in methanol and stirred for 10 min. Added 20% (0.5 ml) aq. NaOH solution to the reaction mixture. After 10 min, added, substituted acetophenone (1 eq) to the reaction mixture and stirred it for 4–6 h. The progress of the reaction was monitored by a TLC plate and visualized under UV light. On the completion of the

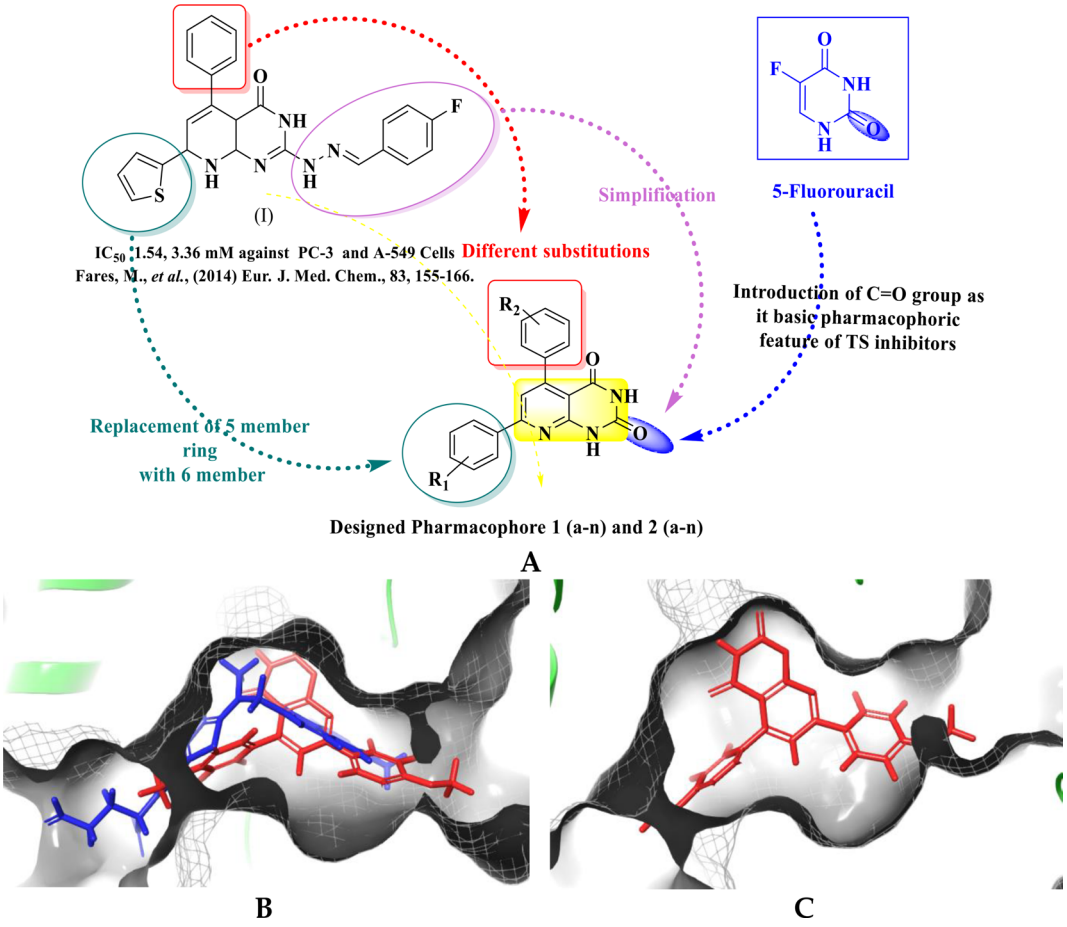

Fig. 1 Design of proposed compounds: **(A)** Design of basic pharmacophore based on reported pyrido[2,3-*d*]pyrimidine derivatives along with 5-fluorouracil; **(B)** Overlay of docked raltitrexed (blue) and structure of compound 1n (red); **(C)** 3D-interaction diagram of the compound 1n inside catalytic pocket of human thymidylate synthase (PDB: 1HVY)

Table 1 Dock score of reported pyrido[2,3-*d*]pyrimidine derivative I and designed compound 2a, raltitrexed and 5-FU

Code	Docking Score (kcal/mol)
I	-6.8 Kcal/mol
1n	-10.6 Kcal/mol
5-FU	-5.4 Kcal/mol
Ral	-9.4 Kcal/mol

reaction, the reaction mixture was filtered, washed, and then crystallized using methanol [11].

(*E*)-1-(4-methoxyphenyl)-3-(naphthalen-2-yl)prop-2-en-1-one

Yield 90.1%; yellowish white powder; m.p.: 140–142 °C; IR (cm^{-1}) ν_{max}: 3055 (C-H_{ar}), 2360 (C=C), 1650 (C=O); ^{1}H NMR (600 MHz, $CDCl_3$) δ (ppm): 8.08 (d, J=8.8 Hz, 2H, H-2', H-6'), 8.03 (d, J=5.8 Hz, 2 H, H-3', H-5'), 7.95 (s, 1H, H-1), 7.88–7.86 (m, 2 H, H-7, H-8), 7.85 (d, J=1.2 Hz, 1H, H-3), 7.84 (d, J=4.9 Hz, 1H, H-4) 7.81–7.78 (m, 2 H, H-5, H-6), 7.66 (d, J=15.6 Hz, 1H, H-β), 7.00 (d, J=8.8 Hz, 1H, H-α), 3.90 (s, 3 H, H-7'); ^{13}C NMR (150 MHz, $CDCl_3$) δ (ppm): 188.6 (C=O), 155.4 (C-4'), 144.1 (C-β), 143.5 (C-2), 134.4 (C-10), 133.5 (C-1'), 130.9 (C-2'), 130.6 (C-1), 130.4 (C-5), 128.7 (C-7), 127.8 (C-6), 127.3 (C-3), 126.8 (C-α), 125.8 (C-1), 123.8 (C-8), 122.1 (C-4), 113.9 (C-3'), 55.6 (C-5'); GCMS (EI) calculated for $C_{20}H_{16}O_2$, 288.11 $[M]^+$; observed: 288.15.

General procedure for the synthesis of diaryl based pyrido[2,3-d]pyrimidines 1(a-n)

In a 100 ml RBF, substituted chalcone (II, 1 Eq) was dissolved in pure methanol and stirred for 20 min. 40% aq NaOH (0.8 ml) solution was added to the reaction mixture. After 15 min, the previously synthesized intermediate I (1 eq.) was put into the reaction mixture and refluxed for 14–16 h. The progress of the reaction was monitored by a TLC plate and visualized under UV light. On the completion of the reaction, the mixture was filtered, washed, and then crystallized using methanol. [11].

5-(4-chlorophenyl)-7-(p-tolyl)pyrido[2,3-*d*] pyrimidine-2,4(1 H,3 H)-dione 1 (a)

Yield: 84.2%; yellow powder; m.p.: 158–160 °C; IR (cm^{-1}) ν_{max}: 3727 (NH), 3432 (NH), 3251 (C-$H_{ar.}$), 2922 (C-$H_{aliph.}$), 2360 (C=C), 1619 (C=O); ^{1}H NMR (600 MHz, DMSO-d_6) δ (ppm): 11.67 (s, 1H, H-1), 11.20 (s, 1H, H-3), 8.11 (d, J=8.4 Hz, 2H, H-2', H-3'), 7.51 (s, 1H, H-6), 7.46 (d, J=4.0 Hz, 4 H, H-4', H-5', H-2", H3"), 7.34 (d, J=8.5 Hz, 2 H, H-4", H-5"), 2.38 (s, 3 H, H-7'); ^{13}C NMR (150 MHz, DMSO-d_6) δ (ppm): 161.9 (C-4), 159.4 C-2), 154.0 (C-5), 152.8 (C-9), 150.7 (C-7), 141.1 (C-1"), 138.2 (C-1'), 134.4 (C-4"), 133.3 (C-4'), 131.0 (C-3'), 130.01 (C-3"), 127.9 (C-2"), 127.9 (C-2'), 117.9 (C-6), 106.0 (C-10), 21.4 (C-5'); GCMS (EI) calculated for $C_{20}H_{14}ClN_3O_2$, 363.80 $[M]^+$; observed: 364 [M+1].

5-(4-chloro-3-fluorophenyl)-7-(p-tolyl)pyrido[2,3-*d*] pyrimidine-2,4(1 H,3 H)-dione 1 (b)

Yield: 56.6%; yellowish brown; m.p.: 178–180 °C; IR (cm^{-1}) ν_{max}: 3729 (NH), 3600 (NH), 3100 (C-$H_{ar.}$), 2919 (C-$H_{aliph.}$), 2360 (C=C), 1716 (C=O); ^{1}H NMR (600 MHz, DMSO-d_6) δ (ppm): 11.61 (s, 1H, H-1), 11.15 (s, 1H, H-3), 8.05 (s, 1H, H-6), 7.49 (s, 1H, H-3"), 7.45 (d, J=3.9 Hz, 1H, H-4"), 7.43 (d, J=1.8 Hz, 1H, H-2"), 7.27 (d, J=5.4 Hz, 2 H, H-2', H-3'), 7.22 (d, J=8.3 Hz, 2 H, H-4', H-5'), 2.32 (s, 3 H, H-7'); ^{13}C NMR (150 MHz, DMSO-d_6) δ (ppm): 161.7 (C-4), 159.7 C-2), 157.7 (C-5"), 153.7 (C-9), 151.5 (C-5), 150.5 (C-7), 141.2 (C-1"), 140.4 (C-1'), 137.4(C-4"), 134.3 (C-3'), 129.9 (C-2'), 127.8 (C-2"), 127.6 (C-4'), 126.3 (C-6"), 119.5 (C-3"), 117.6 (C-6), 105.9 (C-10), 21.2 (C-5'); GCMS (EI) calculated for $C_{20}H_{13}ClFN_3O_2$, 381.06 $[M]^+$; observed: 381.

5-(4-(dimethylamino)phenyl)-7-(p-tolyl)pyrido[2,3-*d*] pyrimidine-2,4(1 H,3 H)-dione 1 (c)

Yield: 55.6%; yellowish brown; m.p.: 172–174 °C; IR (cm^{-1}) ν_{max}: 3728 (NH), 3550 (NH), 3174 (C-$H_{ar.}$), 2922 (C-$H_{aliph.}$), 2360 (C=C), 1713 (C=O); ^{1}H NMR (600 MHz, DMSO-d_6) δ (ppm): 11.51 (s, 1H, H-1), 11.08 (s, 1H, H-3), 8.08 (d, J=10.4 Hz, 2H, H-2', H-3'), 7.44 (s, 1H, H-6), 7.33 (d, J=2.5 Hz, 2 H, H-4", H-5"), 6.79 (d, J=9.0 Hz, 1H, H-3"), 6.73 (d, J=4.8 Hz, 2 H, H-4', H-5'), 6.55 (d, J=1.8 Hz, 1H, H-2"), 2.98 (s, 6 H, H-7", H-8"), 2.38 (s, 3 H, H-7'); ^{13}C NMR (150 MHz, DMSO-d_6) δ (ppm): 162.1 (C-4), 158.8 (C-2), 154.7 (C-4"), 140.8 (C-5), 134.7 (C-9), 130.7 (C-3'), 129.9 (C-2"), 129.5 (C-7), 128.6 (C-1'), 127.9 (C-1"), 127.8 (C-2'), 127.3 (C-3"), 117.9 (C-4'), 113.0 (C-10), 105.6 (C-6), 29.5 (C-5"), 21.6 (C-5'); GCMS (EI) calculated for $C_{22}H_{20}N_4O_2$, 372.15 $[M]^+$; observed: 372.

5-(3,4-dimethoxyphenyl)-7-(p-tolyl)pyrido[2,3-*d*] pyrimidine-2,4(1 H,3 H)-dione 1 (d)

Yield: 53.0%; pale yellow; m.p.: 182–184 °C; IR (cm^{-1}) ν_{max}: 3728 (NH), 3600 (NH), 3100 (C-$H_{ar.}$), 2923 (C-$H_{aliph.}$), 2360 (C=C), 1713 (C=O); ^{1}H NMR (600 MHz, DMSO-d_6) δ (ppm): 11.57 (s, 1H, H-1), 11.13 (s, 1H, H-3), 8.10 (d, J=6.2 Hz, 2H, H-2', H-3'), 7.50 (s, 1H, H-6), 7.34 (d, J=3.6 Hz, 1H, H-2"), 7.33 (d, J=4.2 Hz, 1H, H-4"), 7.06 (s, 1H, H-3"), 6.98 (d, J=2.0 Hz, 2 H, H-4', H-5'), 3.82 (s, 3 H, H-8"), 3.76 (s, 3 H, H-7"), 2.37 (s, 3 H, H-7'); ^{13}C NMR (150 MHz, DMSO-d_6) δ (ppm): 161.9 (C-4), 159.1 (C-2), 154.2 (C-9), 154.0 (C-5), 150.7 (C-5"), 149.4 (C-6"), 148.2 (C-7), 140.9 (C-1"), 134.6 (C-1'), 131.7 (C-4'), 129.9 (C-3'), 127.8 (C-2'), 121.8 (C-2"), 118.1 (C-3"), 113.8 (C-4"), 111.3 (C-10), 106.1 (C-6), 56.1 (C-7"), 56.0 (C-8"), 21.4 (C-5'); GCMS (EI) calculated for $C_{22}H_{19}N_3O_4$, 389.13 $[M]^+$; observed: 389.

5-(2,6-dichlorophenyl)-7-(p-tolyl)pyrido[2,3-*d*] pyrimidine-2,4(1 H,3 H)-dione 1 (e)

Yield: 42.7%; golden brown; m.p.: 180–182 °C; IR (cm^{-1}) ν_{max}: 3729 (NH), 3600 (NH), 3171 (C-$H_{ar.}$), 2921 (C-$H_{aliph.}$), 2360 (C=C), 1675 (C=O); ^{1}H NMR (600 MHz, DMSO-d_6) δ (ppm): 11.84 (s, 1H, H-1), 11.32 (s, 1H, H-3), 8.13 (d, J=3.8 Hz, 1H, H-3'), 8.12 (s, 1H, H-6), 7.63 (d, J=3.5 Hz, 1H, H-2'), 7.56 (d, J=3.3 Hz, 1H, H-4"), 7.55 (d, J=3.7 Hz, 1H, H-5"), 7.45 (dd, J=8.4, 3.2 Hz, 1H, H-6"), 7.34 (d, J=8.1 Hz, 2 H, H-4', H-5'), 2.37 (s, 3 H, H-7'); ^{13}C NMR (150 MHz, DMSO-d_6) δ (ppm): 161.9 (C-4), 159.4 (C-2), 154.0 (C-5), 152.8 (C-9), 150.7 (C-7), 141.1 (C-1"), 138.2 (C-1'), 134.4 (C-4"), 133.3 (C-4'), 131.0 (C-2"), 130.0 (C-3'), 127.9 (C-3"), 127.9 (C-2'), 117.9 (C-10), 106.0 (C-6), 21.4 (C-5'); GCMS (EI) calculated for $C_{20}H_{13}Cl_2N_3O_2$, 397.03 $[M]^+$; observed: 396 [M−1].

5-(3-bromophenyl)-7-(4-methoxyphenyl)pyrido[2,3-*d*] pyrimidine-2,4(1 H,3 H)-dione 1 (f)

Yield: 62.7%; pale yellow; m.p.: 170–172 °C; IR (cm^{-1}) ν_{max}: 3729 (NH), 3600 (NH), 3164 (C-$H_{ar.}$), 2924 (C-$H_{aliph.}$), 2360 (C=C), 1685 (C=O); ^{1}H NMR (600 MHz, DMSO-d_6) δ (ppm): 11.65 (s, 1H, H-1), 11.18 (s, 1H, H-3), 8.20 (d, J=8.9 Hz, 2H, H-2', H-3'), 7.62 (s, 1H, H-6), 7.60 (d, J=7.9 Hz, 1H, H-2"), 7.50 (s, 1H, H-3"), 7.42 (d, J=7.8 Hz, 1H, H-6"), 7.37 (t, J=7.7 Hz, 1H, H-4"), 7.07 (d, J=8.9 Hz, 2 H, H-4', H-5'), 3.84 (s, 3 H, H-7'); ^{13}C NMR (150 MHz, DMSO-d_6) δ (ppm): 162.0 (C-4), 161.8 (C-2), 159.4 (C-6'), 153.6 (C-4'), 152.3 (C-5), 150.7 (C-9), 141.5 (C-7), 131.4 (C-1"), 131.2 (C-3"), 130.2 (C-4"), 129.7 (C-2'), 129.3 (C-1'), 127.9 (C-2"), 121.1 (C-5"), 117.4 (C-10), 114.8 (C-3'), 105.3 (C-6), 55.8 (C-5'); GCMS (EI) calculated for $C_{20}H_{14}BrN_3O_3$, 423.02 $[M]^+$; observed: 423.00.

5-(2-chlorophenyl)-7-(4-methoxyphenyl)pyrido[2,3-*d*] pyrimidine-2,4(1 H,3 H)-dione 1 (g)

Yield: 69.3%; light orange; m.p.: 166–168 °C; IR (cm^{-1}) ν_{max}: 3700 (NH), 3600 (NH), 3178 (C-$H_{ar.}$),

2839 (C-$H_{aliph.}$), 2360 (C=C), 1695 (C=O); ^{1}H NMR (600 MHz, DMSO-d_6) δ (ppm): 11.71 (s, 1H, H-1), 11.20 (s, 1H, H-3), 8.20 (d, J=9.0 Hz, 2H, H-2′, H-3′), 7.51 (d, J=1.7 Hz, 1H, H-2″), 7.49 (s, 1H, H-6), 7.45–7.39 (m, 2 H, H-4″, H-6″), 7.35 (d, J=7.0, 2.2 Hz, 1H, H-5″), 7.07 (d, J=8.9 Hz, 2 H, H-4′, H-5′), 3.84 (s, 3 H, H-7′); ^{13}C NMR (150 MHz, DMSO-d_6) δ (ppm): 162.0 (C-4), 161.6 (C-2), 159.7 (C-4′), 153.5 (C-5), 150.85 (C-9), 150.7 (C-7), 138.8 (C-1″), 131.8 (C-3″), 130.0 (C-2′), 129.8 (C-2″), 129.7 (C-6″), 129.4 (C-5″), 129.0 (C-4″), 127.2(C-1′), 116.9 (C-10), 114.8 (C-3′), 114.7 (C-6), 55.9 (C-5′); GCMS (EI) calculated for $C_{20}H_{14}ClN_3O_3$, 379.07 $[M]^+$; observed: 379.10.

5-(4-bromophenyl)-7-(4-methoxyphenyl)pyrido[2,3-*d*] pyrimidine-2,4(1 H,3 H)-dione 1(h)

Yield: 58%; pale yellow; m.p.: 171–173 °C; IR (cm^{-1}) ν_{max}: 3720 (NH), 3600 (NH), 3177 (C-$H_{ar.}$), 2839 (C-$H_{aliph.}$), 2360 (C=C), 1698 (C=O); ^{1}H NMR (600 MHz, DMSO-d_6) δ (ppm): 11.65 (s, 1H, H-1), 11.18 (s, 1H, H-3), 8.18 (d, J=9.0 Hz, 2H, H-2′, H-3′), 7.60 (d, J=8.4 Hz, 2 H, H-4″, H-5″), 7.47 (s, 1H, H-6), 7.38 (d, J=8.4 Hz, 2 H, H-2″, H-3″), 7.07 (d, J=9.0 Hz, 2 H, H-4′, H-5′), 3.84 (s, 3 H, H-7′); ^{13}C NMR (150 MHz, DMSO-d_6) δ (ppm): 161.9 (C-4, C-4′), 159.2 (C-2), 153.9 (C-5), 152.7 (C-9), 150.7 (C-7), 138.7 (C-4″), 131.3 (C-2″), 130.8 (C-2′), 129.6 (C-3″), 129.5 (C-1″), 121.9 (C-1′), 117.3 (C-10), 114.7 (C-3′), 105.4 (C-6), 55.9 (C-5′); GCMS (EI) calculated for $C_{20}H_{14}BrN_3O_3$, 423.02 $[M]^+$; observed: 423.00.

5-(4-chlorophenyl)-7-(4-methoxyphenyl)pyrido[2,3-*d*] pyrimidine-2,4(1 H,3 H)-dione 1 (i)

Yield: 67%; pale yellow; m.p.: 164–166 °C; IR (cm^{-1}) ν_{max}: 3729 (NH), 3600 (NH), 3200 (C-$H_{ar.}$), 2900 (C-$H_{aliph.}$), 2360 (C=C), 1702 (C=O); ^{1}H NMR (600 MHz, DMSO-d_6) δ (ppm): 11.65 (s, 1H, H-1), 11.18 (s, 1H, H-3), 8.18 (d, J=8.9 Hz, 2H, H-2′, H-3′), 7.47 (s, 1H, H-6), 7.46–143 (m, 3 H, H-3″, H-4″, H-5″), 7.43 (d, J=2.4 Hz, 1H, H-2″), 7.07 (d, J=9.0 Hz, 2 H, H-4′, H-5′), 3.84 (s, 3 H, H-7′); ^{13}C NMR (150 MHz, DMSO-d_6) δ (ppm): 161.9 (C-4, C-4′), 159.2 (C-2), 153.9 (C-5), 152.7 (C-9), 150.6 (C-7), 138.3 (C-4″), 133.2 (C-1″), 131.0 (C-1′), 129.6 (C-2″), 129.5 (C-2′), 127.8 (C-3″), 117.4 (C-10), 114.7 (C-3′), 105.5 (C-6), 55.9 (C-5′); GCMS (EI) calculated for $C_{20}H_{14}ClN_3O_3$, 379.07 $[M]^+$; observed: 379.10.

5-(4-(dimethylamino)phenyl)-7-(4-methoxyphenyl) pyrido[2,3-*d*]pyrimidine-2,4(1 H,3 H)-dione 1(j)

Yield: 72%; yellowish brown; m.p.: 158–160 °C; IR (cm^{-1}) ν_{max}: 3729 (NH), 3600 (NH), 3200 (C-$H_{ar.}$), 2924 (C-$H_{aliph.}$), 2360 (C=C), 1701 (C=O); ^{1}H NMR (600 MHz, DMSO-d_6) δ (ppm): 11.50 (s, 1H, H-1), 11.07 (s, 1H, H-3), 8.16 (d, J=9.0 Hz, 2H, H-2′, H-3′), 7.41 (s, 1H, H-6), 7.32 (d, J=8.8 Hz, 2 H, H-2″, H-3″), 7.07 (d, J=8.9 Hz, 2 H, H-4′, H-5′), 6.73 (d, J=8.9 Hz, 2 H, H-4″, H-5″), 3.84 (s, 3 H, H-7′), 2.97 (s, 6 H, H-7″, H-8″); ^{13}C NMR (150 MHz, DMSO-d_6) δ (ppm): 162.1 (C-4), 161.7 (C-2), 158.6 (C-4′), 154.6 (C-4″), 154.2 (C-5), 150.9 (C-9), 150.7 (C-7), 130.6 (C-2′), 129.9 (C-2″), 129.4 (C-1″), 126.4 (C-1′), 117.4 (C-10), 114.7 (C-3′), 111.4 (C-3″), 105.1 (C-6), 55.8 (C-5′), 40.6 (C-5″); GCMS (EI) calculated for $C_{22}H_{20}N_4O_3$, 388.42 $[M]^+$; observed: 388.

5-(2,6-dimethoxyphenyl)-7-(4-methoxyphenyl) pyrido[2,3-*d*]pyrimidine-2,4(1 H,3 H)-dione 1(k)

Yield: 55%; creamish white; m.p.: 168–170 °C; IR (cm^{-1}) ν_{max}: 3700 (NH), 3600 (NH), 3167 (C-$H_{ar.}$), 2834 (C-$H_{aliph.}$), 2360 (C=C), 1682 (C=O); ^{1}H NMR (600 MHz, DMSO-d_6) δ (ppm): 11.57 (s, 1H, H-1), 11.08 (s, 1H, H-3), 8.17 (d, J=8.9 Hz, 2H, H-2′, H-3′), 7.44 (s, 1H, H-6), 7.08 (d, J=5.0 Hz, 2 H, H-4′, H-5′), 6.97–6.90 (m, 2 H, H-4″, H-5″), 6.81 (t, J=2.6 Hz, 1H, H-6″), 3.84 (s, 3 H, H-7′), 3.74 (s, 3 H, H-7″), 3.60 (s, 3 H, H-8″); ^{13}C NMR (150 MHz, DMSO-d_6) δ (ppm): 161.8 (C-4), 159.3 (C-2), 153.3 (C-4′), 153.3 (C-2″), 150.7 (C-5), 150.7 (C-9), 129.6 (C-2′), 129.5 (C-3′), 117.5 (C-7), 117.5 (C-1′), 115.5 (C-10), 115.4 (C-1″), 114.7 (C-3″), 114.7(C-4″), 114.1 (C-6), 56.4 (C-5″), 55.9 (C-5′); GCMS (EI) calculated for $C_{22}H_{19}N_3O_5$, 405.13 $[M]^+$; observed: 405.

5-(2,5-dimethoxyphenyl)-7-(4-methoxyphenyl) pyrido[2,3-*d*]pyrimidine-2,4(1 H,3 H)-dione 1(l)

Yield: 62%; pale yellow; m.p.: 168–170 °C; IR (cm^{-1}) ν_{max}: 3729 (NH), 3600 (NH), 3177 (C-$H_{ar.}$), 2921 (C-$H_{aliph.}$), 2360 (C=C), 1703 (C=O); ^{1}H NMR (600 MHz, DMSO-d_6) δ (ppm): 11.53 (s, 1H, H-1), 11.05 (s, 1H, H-3), 8.15 (d, J=8.9 Hz, 2H, H-2′, H-3′), 7.40 (s, 1H, H-6), 7.14 (d, J=8.9 Hz, 1H, H-5″), 7.06 (d, J=8.9 Hz, 2 H, H-4′, H-5′), 6.59 (s, 1H, H-2″), 6.57 (d, J=4.4 Hz, 1H, H-6″), 3.84 (s, 3 H, H-7′), 3.82 (s, 3 H, H-7″), 3.65 (s, 3 H, H-8″); ^{13}C NMR (150 MHz, DMSO-d_6) δ (ppm): 161.8 (C-4), 161.7 (C-2), 161.3 (C-4′), 159.2 (C-4″), 158.1 (C-3″), 153.3 (C-5), 150.8 (C-9), 150.7 (C-7), 132.0 (C-1′), 130.0 (C-1″), 129.7 (C-6″), 129.5 (C-2″), 129.2 (C-2′), 117.8 (C-5″), 114.7 (C-3′), 106.9 (C-6), 104.8 (C-10), 55.9 (C-7″), 55.8 (C-8″), 55.8 (C-5′); GCMS (EI) calculated for $C_{22}H_{19}N_3O_5$, 405.13 $[M]^+$; observed: 405.

5-(4-methoxyphenyl)-7-(4-methoxyphenyl)pyrido[2,3-*d*] pyrimidine-2,4(1 H,3 H)-dione 1(m)

Yield: 63%; pale yellow; m.p.: 158–160 °C; IR (cm^{-1}) ν_{max}: 3729 (NH), 3600 (NH), 3164 (C-$H_{ar.}$), 2919 (C-$H_{aliph.}$), 2360 (C=C), 1615 (C=O); ^{1}H NMR (600 MHz, DMSO-d_6) δ (ppm): 11.57 (s, 1H, H-1), 11.07 (s, 1H, H-3), 8.17 (d, J=8.9 Hz, 2H, H-2′, H-3′), 8.13 (d, J=9.0 Hz, 1H, H-2″), 7.43 (s, 1H, H-6), 7.20 (d, J=7.4, 1.8 Hz, 1H, H-3″), 7.06 (d, J=9.0 Hz, 2 H,, , H-4′, H-5′), 7.04 (d, J=1.2 Hz, 1H, H-4″), 7.02 (d, J=2.9 Hz, 1H, H-5″), 3.84 (s, 3 H, H-7′), 3.66 (s,

3 H, H-7"); ^{13}C NMR (150 MHz, DMSO-d_6) δ (ppm): 161.8 (C-4), 161.6 (C-2), 159.3 (C-5'), 156.8 (C-5"), 153.3 (C-5), 151.0 (C-9), 150.7 (C-7), 129.9 (C-1'), 129.6 (C-1"), 129.5 (C-2'), 129.3(C-3"), 129.0 (C-2"), 120.5 (C-4'), 117.5 (C-4"), 114.7 (C-3'), 111.1 (C-10), 106.8 (C-5), 55.9 (C-6', C-6"); GCMS (EI) calculated for $C_{21}H_{17}N_3O_4$, 375.12 $[M]^+$; observed: 375.

7-(4-methoxyphenyl)-5-(naphthalen-2-yl)pyrido[2,3-*d*]pyrimidine-2,4(1 H,3 H)-dione 1 (n)

Yield: 70.1%; % Purity≥98 (HPLC); light brown; m.p.: 176–178 °C; IR (cm^{-1}) ν_{max}: 3700 (NH), 3600 (NH), 3176 (C-$H_{ar.}$), 2920 (C-$H_{aliph.}$), 2360 (C=C), 1703 (C=O); ^{1}H NMR (600 MHz, DMSO-d_6) δ (ppm): 11.62 (s, 1H, H-1), 11.15 (s, 1H, H-3), 8.18 (d, *J*=8.9 Hz, 2H, H-2', H-3'), 7.95–7.92 (m, 3 H, H-7", H-8", H-1"), 7.87 (d, *J*=8.5 Hz, 1H, H-5"), 7.55 (d, *J*=3.8 Hz, 2 H, H-4', H-5'), 7.54 (s, 1H, H-6), 7.51 (dd, *J*=8.4, 1.8 Hz, 1H, H- H-6"'), 7.04 (d, *J*=8.9 Hz, 2 H, H-3", H-4"), 3.85 (s, 3 H, H-7'); ^{13}C NMR (150 MHz, DMSO-d_6) δ (ppm): 161.9 (C-4), 161.9 (C-2), 159.3 (C-4') 154.0 (C-5), 150.8 (C-9), 137.5 (C-7), 133.0 (C-2"), 129.7 (C-8"), 129.5 (C-2'), 128.5 (C-6"), 127.8 (C-7"), 127.1 (C-1'), 127.1 (C-1"), 126.6 (C-4"), 126.6 (C-3"), 126.5 (C-10), 117.7 (C-5"), 114.6 (C-3'), 105.6 (C-5), 55.7 (C-5'); GCMS (EI) calculated for $C_{24}H_{17}N_3O_3$, 395.12 $[M]^+$; observed: 395.15; HRMS (TOF MS) calculated for $C_{24}H_{17}N_3O_3$, 396.1348 [M+H]; observed: 396.1357 [M+H].

General procedure for the synthesis of alkyl substituted pyrido[2,3-d]pyrimidine derivatives 2 (a-n)

In a round bottom flask, potassium hydroxide (4 eq) in acetonitrile 25 ml was stirred for 10–15 min. Diaryl-based pyrido[2,3-*d*]pyrimidines 1(a-n) (1 eq) was added to the solution, and then the reaction mixture was stirred for 20–25 min at 0–4 °C. Then methyl iodide (2.5 eq) [11] was added to the stirred mixture. The reaction was monitored by TLC. After the completion of the reaction (2–4 h), a workup was done using ethyl acetate and water, and the final product was purified by column chromatography.

5-(4-chlorophenyl)-1,3-dimethyl-7-(p-tolyl)pyrido[2,3-*d*]pyrimidine-2,4(1 H,3 H)-dione 2 (a)

Yield: 86.1%; light brown; m.p.: 164–166 °C; IR (cm^{-1}) ν_{max}: 3200 (C-$H_{ar.}$), 2924 (C-$H_{aliph.}$), 2360 (C=C), 1710 (C=O); ^{1}H NMR (600 MHz, $CDCl_3$) δ (ppm): 7.97 (d, J=8.3 Hz, 2H, H-2', H-3'), 7.42 (d, J=8.5 Hz, 2 H, H-2", H-3"), 7.38 (d, J=8.6 Hz, 2 H, H-4", H-5"), 7.26–7.24 (m, 2 H, H-4', H-5'), 6.91 (s, 1H, H-6), 3.11 (s, 3 H, H-1), 2.63 (s, 3 H, H-3), 2.40 (s, 3 H, H-7'); ^{13}C NMR (150 MHz, $CDCl_3$) δ (ppm): 169.3 (C-4), 157.5 (C-2), 156.6 (C-9), 147.4 (C-1"), 139.4 (C-1'), 138.1 (C-4"), 136.3 (C-4'), 134.8, 129.6 (C-3'), 129.3 (C-2"), 129.1 (C-3"), 126.9 (C-7), 117.9, 110.9 (C-6), 108.8 (C-10), 28.3 (C-1), 26.5 (C-3), 21.4 (C-5'); GCMS (EI) calculated for $C_{22}H_{18}ClN_3O_2$, 391.10 $[M]^+$; observed: 391.35.

5-(4-chloro-3-fluorophenyl)-1,3-dimethyl-7-(p-tolyl)pyrido[2,3-*d*]pyrimidine-2,4(1 H,3 H)-dione 2 (b)

Yield: 81.1%; brown; m.p.: 180−122 °C; IR (cm^{-1}) ν_{max}: 3251 (C-$H_{ar.}$), 2922 (C-$H_{aliph.}$), 2360 (C=C), 1619 (C=O); ^{1}H NMR (600 MHz, $CDCl_3$) δ (ppm): 7.96 (d, J=8.1 Hz, 2H, H-2', H-3'), 7.45 (t, J=7.8 Hz, 1H, H-4"), 7.27 (d, J=1.9 Hz, 1H, H-3"), 7.16 (dd, J=8.2, 1.5 Hz, 2 H, H-4', H-5'), 6.88 (s, 1H, H-6), 6.46 (d, J=4.5 Hz, 1H, H-2"), 3.10 (s, 3 H, H-1), 2.65 (s, 3 H, H-3), 2.39 (s, 3 H, H-7'); ^{13}C NMR (150 MHz, $CDCl_3$) δ (ppm): 169.0 (C-4), 159.0 (C-2), 157.4 (C-5"), 156.8 (C-9), 146.3 (C-5), 140.2 (C-7), 139.5 (C-1"), 136.1 (C-1'), 131.0 (C-4"), 129.4 (C-2'), 126.9 (C-3'), 124.8 (C-4'), 121.4 (C-2"), 116.5 (C-2"), 116.3 (C-3"), 110.9 (C-6), 108.5 (C-10), 28.4 (C-1), 26.6 (C-3), 21.4 (C-5'); GCMS (EI) calculated for $C_{22}H_{17}ClFN_3O_2$, 409.09 $[M]^+$; observed: 409.

5-(4-(dimethylamino)phenyl)-1,3-dimethyl-7-(p-tolyl)pyrido[2,3-*d*]pyrimidine-2,4(1 H,3 H)-dione 2 (c)

Yield: 87%; dark brown; m.p.: 176–178 °C; IR (cm^{-1}) ν_{max}: 2972 (C-$H_{aliph.}$), 2360 (C=C), 1698 (C=O); ^{1}H NMR (600 MHz, $CDCl_3$) δ (ppm): 8.03 (d, J=8.2 Hz, 2H, H-4', H-5'), 7.45 (s, 1H, H-6,), 7.30 (d, J=8.7 Hz, 4 H, H-2", H-3", H-2', H-3'), 6.79 (d, J=8.7 Hz, 2 H, H-4", H-5"), 3.86 (s, 3 H, H-1), 3.41 (s, 3 H, H-3), 3.03 (s, 6 H, H-7", H-8"), 2.43 (s, 3 H, H-7'); ^{13}C NMR (150 MHz, $CDCl_3$) δ (ppm): 160.8 (C-4), 158.8 (C-2), 155.7 (C-4"), 152.1 (C-9), 151.8 (C-5), 150.6 (C-7), 140.9 (C-1'), 134.9 (C-1"), 129.7 (C-3'), 129.6 (C-2"), 127.4 (C-2'), 126.7 (C-4'), 118.4 (C-6), 111.3 (C-3"), 106.2 (C-10), 40.4 (C-5"), 30.2 (C-1), 28.5 (C-3), 21.5 (C-5'); GCMS (EI) calculated for $C_{24}H_{24}N_4O_2$, 400.18 $[M]^+$; observed: 400.

5-(3,4-dimethoxyphenyl)-1,3-dimethyl-7-(p-tolyl)pyrido[2,3-*d*]pyrimidine-2,4(1 H,3 H)-dione 2 (d)

Yield: 86%; yellowish brown; m.p.: 184–186 °C; IR (cm^{-1}) ν_{max}: 3381 (=C-$H_{ar.}$), 2942 (C-$H_{aliph.}$), 2360 (C=C), 1708 (C=O); ^{1}H NMR (600 MHz, $CDCl_3$) δ (ppm): 7.99 (d, J=8.1 Hz, 2H, H-2', H-3'), 7.24 (s, 1H, H-6), 7.03 (dd, J=8.2, 2.0 Hz, 1H, H-2"), 6.95 (d, J=3.1 Hz, 2 H, H-4', H-5'), 6.93 (d, J=2.2 Hz, 1H, H-4"), 6.68 (s, 1H, H-3"), 3.93 (s, 3 H, H-8"), 3.90 (s, 3 H, H-7"), 3.12 (s, 3 H, H-1), 2.63 (s, 3 H, H-3), 2.40 (s, 3 H, H-7'); ^{13}C NMR (150 MHz, $CDCl_3$) δ (ppm): 169.8 (C-4), 157.6 (C-2), 156.4 (C-6"), 149.4 (C-5"), 149.2 (C-9), 148.7 (C-5), 139.2 (C-7), 136.5 (C-1'), 132.3 (C-1"), 129.3 (C-2'), 126.9 (C-4'), 120.6) (C-3'), 118.3 (C-2", 111.8 (C-3"), 111.4 (C-6), 110.7 (C-4"), 109.1 (C-10), 56.0 (C-7", C-8"), 28.3 (C-1), 26.6 (C-3), 21.4 (C-5'); GCMS (EI) calculated for $C_{24}H_{23}N_3O_4$, 417.16 $[M]^+$; observed: 417.

5-(2,6-dichlorophenyl)-1,3-dimethyl-7-(p-tolyl) pyrido[2,3-*d*]pyrimidine-2,4(1 H,3 H)-dione 2 (e)
Yield: 79%; dark brown; m.p.: 188–190 °C; IR (cm^{-1}) ν_{max}: 2942 (C-$H_{aliph.}$), 2360 (C=C), 1697 (C=O); ^{1}H NMR (600 MHz, $CDCl_3$) δ (ppm): 7.96 (d, J=1.8 Hz, 2H, H-2', H-3'), 7.55 (d, J=8.0 Hz, 1H, H-6"), 7.29 (d, J=3.1 Hz, 2 H, H-4', H-5'), 7.25 (s, 1H, H-6), 7.07 (d, J=8.0 Hz, 1H, H-5"), 6.91 (d, J=7.9 Hz, 1H, H-4"), 3.12 (s, 3 H, H-1), 2.95 (s, 3 H, H-3), 2.43 (s, 3 H, H-7'); ^{13}C NMR (150 MHz, $CDCl_3$) δ (ppm): 161.5 (C-4), 158.5 (C-2), 151.3 (C-9), 146.5 (C-5), 139.4 (C-7), 138.3 (C-1'), 135.6 (C-1"), 132.6 (C-4'), 129.7 (C-2"), 128.4, (C-4") 128.1 (C-3'), 128.0 (C-6), 127.0 (C-3"), 125.2 (C-2'), 108.1 (C-10), 31.0 (C-1), 28.0 (C-3), 21.3 (C-5'); GCMS (EI) calculated for $C_{22}H_{17}Cl_2N_3O_2$, 425.06 $[M]^+$; observed: 427.15 [M+2].

5-(3-bromophenyl)-7-(4-methoxyphenyl)-1,3-dimethylpyrido[2,3-*d*]pyrimidine-2,4(1 H,3 H)-dione 2 (f)
Yield: 82%; brown; m.p.: 178–180 °C; IR (cm^{-1}) ν_{max}: 3391 (=C-$H_{ar.}$), 2945 (C-$H_{aliph.}$), 2360 (C=C), 1697 (C=O); ^{1}H NMR (600 MHz, $CDCl_3$) δ (ppm): 8.05 (d, J=8.8 Hz, 2H, H-2', H-3'), 7.63–7.62 (m, 2 H, H-4", H-6"), 7.36 (d, J=6.4 Hz, 1H, H-3"), 7.31 (s, 1H, H-6), 6.97 (d, J=8.8 Hz, 2 H, H-4', H-5'), 6.87 (s, 1H, H-2"), 3.86 (s, 3 H, H-7'), 3.11 (s, 3 H, H-1), 2.63 (s, 3 H, H-3); ^{13}C NMR (150 MHz, $CDCl_3$) δ (ppm): 160.8 (C-4), 157.5 (C-2), 156.3 (C-9), 147.2 (C-5), 141.9 (C-1'), 131.7 (C-1"), 131.0 (C-4'), 130.3 (C-2"), 129.2 (C-3'), 128.4 (C-4"), 127.1 (C-3"), 122.9 (C-7), 117.3 (C-6"), 114.4 (C-5"), 114.0 (C-2'), 110.3 (C-10), 108.3 (C-6), 55.4 (C-5'), 28.3 (C-1), 26.5 (C-3); GCMS (EI) calculated for $C_{22}H_{18}BrN_3O_3$, 451.05 $[M]^+$; observed: 451.00.

5-(2-chlorophenyl)-7-(4-methoxyphenyl)-1,3-dimethylpyrido[2,3-*d*]pyrimidine-2,4(1 H,3 H)-dione 2 (g)
Yield: 86%; yellowish brown; m.p.: 170–172 °C; IR (cm^{-1}) ν_{max}: 2941 (C-$H_{aliph.}$), 2360 (C=C), 1697 (C=O); ^{1}H NMR (600 MHz, $CDCl_3$) δ (ppm): 8.12 (d, J=8.9 Hz, 2H, H-2', H-3'), 7.96 (d, J=8.9 Hz, 1H, H-3"), 7.50 (d, J=9.1 Hz, 1H, H-5"), 7.37 (s, 1H, H-6), 7.02 (d, J=8.9 Hz, 2 H, H-4', H-5'), 6.91 (d, J=8.8 Hz, 2 H, H-4", H-6"), 3.89 (s, 3 H, H-7'), 3.86 (s, 3 H, H-1), 3.38 (s, 3 H, H-3); ^{13}C NMR (150 MHz, $CDCl_3$) δ (ppm): 162.1 (C-4), 159.5 (C-2), 151.6 (C-9), 138.9 (C-5), 132.1 (C-1'), 130.5 (C-1"), 129.4 (C-4'), 129.2 (C-2'), 128.7 (C-3"), 128.4 (C-2"), 127.7 (C-4"), 127.0 (C-7), 126.6 (C-5"), 116.9 (C-6"), 114.4 (C-3'), 113.8 (C-10), 109.1 (C-6), 55.5 (C-5'), 30.1 (C-1), 28.4 (C-3); GCMS (EI) calculated for $C_{22}H_{18}ClN_3O_3$, 407.85 $[M]^+$; observed: 407.15.

5-(4-bromophenyl)-7-(4-methoxyphenyl)-1,3-dimethylpyrido[2,3-*d*]pyrimidine-2,4(1 H,3 H)-dione 2 (h)
Yield: 88%; brown; m.p.: 175–177 °C; IR (cm^{-1}) ν_{max}: 2962 (C-$H_{aliph.}$), 2360 (C=C), 1698 (C=O); ^{1}H NMR (600 MHz, $CDCl_3$) δ (ppm): 8.11 (d, J=8.9 Hz, 2H, H-2', H-3'), 8.04 (d, J=8.8 Hz, 1H, H-2"), 7.35 (s, 1H, H-6), 7.33–7.32 (m, 1H, H-3"), 7.22 (d, J=8.4 Hz, 2 H, H-4", H-5"), 7.02 (d, J=8.9 Hz, 2 H, H-4', H-5'), 3.87 (s, 3 H, H-7'), 3.11 (s, 3 H, H-1), 2.63 (s, 3 H, H-3); ^{13}C NMR (150 MHz, $CDCl_3$) δ (ppm): 160.6 (C-4), 159.1 (C-2), 153.7 (C-9), 151.6 (C-5), 147.5 (C-4'), 138.6 (C-1"), 132.1 (C-1"), 131.1 (C-2"), 129.6 (C-2'), 129.2 (C-3"), 128.4 (C-4"), 117.3 (C-7), 114.4 (C-3'), 114.0 (C-10), 108.3 (C-6), 55.5 (C-5'), 30.2 (C-1), 28.5 (C-3); GCMS (EI) calculated for $C_{22}H_{18}BrN_3O_3$, 451.05 $[M]^+$; observed: 453.00 [M+2].

5-(4-chlorophenyl)-7-(4-methoxyphenyl)-1,3-dimethylpyrido[2,3-*d*]pyrimidine-2,4(1 H,3 H)-dione 2 (i)
Yield: 81%; yellowish brown; m.p.: 168–170 °C; IR (cm^{-1}) ν_{max}: 2928 (C-$H_{aliph.}$), 2360 (C=C), 1653 (C=O); ^{1}H NMR (600 MHz, $CDCl_3$) δ (ppm): 8.11 (d, J=9.2 Hz, 2H, H-2', H-3'), 8.04 (d, J=9.1 Hz, 2 H, H-2", H-3"), 7.35 (s, 1H, H-6), 7.02 (d, J=9.1 Hz, 2 H, H-4", H-5"), 6.97 (d, J=9.1 Hz, 2 H, H-4', H-5'), 3.89 (s, 3 H, H-7'), 3.10 (s, 3 H, H-1), 2.63 (s, 3 H, H-3); ^{13}C NMR (150 MHz, $CDCl_3$) δ (ppm): 162.1 (C-4), 159.1 (C-2), 156.3 (C-9), 153.7 (C-5), 147.5 (C-4'), 138.1 (C-1'), 130.5 (C-1"), 129.6 (C-2"), 129.2 (C-2'), 128.4 (C-3"), 128.2 (C-4"), 117.4 (C-7), 114.4 (C-3'), 113.8 (C-10), 108.4 (C-6), 55.5 (C-5'), 30.2 (C-1), 28.3 (C-3); GCMS (EI) calculated for $C_{22}H_{18}ClN_3O_3$, 407.85 $[M]^+$; observed: 407.15.

5-(4-(dimethylamino)phenyl)-7-(4-methoxyphenyl)-1,3-dimethylpyrido[2,3-*d*]pyrimidine-2,4(1 H,3 H)-dione 2 (j)
Yield: 90%; % Purity≥98 (HPLC); dark brown; m.p.: 162–164 °C; IR (cm^{-1}) ν_{max}: 2920 (C-$H_{aliph.}$), 2360 (C=C), 1699 (C=O); ^{1}H NMR (600 MHz, $CDCl_3$) δ (ppm): 8.10 (d, J=8.7 Hz, 2H, H-2', H-3'), 7.40 (s, 1H, H-6), 7.29 (d, J=8.6 Hz, 2 H, H-2", H-3"), 7.00 (d, J=8.7 Hz, 2 H, H-4", H-5"), 6.78 (d, J=8.6 Hz, 2 H, H-4', H-5'), 3.88 (s, 3 H, H-7'), 3.85 (s, 3 H, H-1), 3.40 (s, 3 H, H-3), 3.02 (s, 6 H, H-7", H-8"); ^{13}C NMR (150 MHz, $CDCl_3$) δ (ppm): 161.7 (C-4), 160.8 (C-2), 158.3 (C-9), 155.5 (C-5), 150.5 (C-4'), 130.3 (C-6"), 130.1 (C-2'), 129.5 (C-2"), 129.0 (C-7), 126.7 (C-1"), 117.9 (C-1'), 114.2 (C-3'), 113.7 (C-10), 111.2 (C-3"), 105.7 (C-6), 55.4 (C-5'), 40.3 (C-5"), 29.7 (C-1), 28.4 (C-3); GCMS (EI) calculated for $C_{24}H_{24}N_4O_3$, 416.18 $[M]^+$; observed: 416.20; HRMS (TOF MS) calculated for $C_{24}H_{24}N_4O_3$, 417.1926 [M+H]; observed: 417.1941 [M+H].

5-(2,6-dimethoxyphenyl)-7-(4-methoxyphenyl)-1,3-dimethylpyrido[2,3-*d*]pyrimidine-2,4(1 H,3 H)-dione 2 (k)
Yield: 82%; yellowish brown; m.p.: 171–173 °C; IR (cm^{-1}) ν_{max}: 2940 (C-$H_{aliph.}$), 2360 (C=C), 1697 (C=O); ^{1}H NMR (600 MHz, $CDCl_3$) δ (ppm): 8.11 (d, J=8.9 Hz, 2H, H-2', H-3'), 8.04 (d, J=8.8 Hz, 2 H, H-4', H-5'), 7.39

(s, 1H, H-6), 7.00 (d, J=2.3 Hz, 1H, H-5"), 6.8–6.92 (m, 2 H, H-4", H-6"), 3.89 (s, 3 H, H-7'), 3.85 (s, 3 H, H-7"), 3.74 (s, 3 H, H-8"), 3.68 (s, 3 H, H-1), 3.38 (s, 3 H, H-3); ^{13}C NMR (150 MHz, $CDCl_3$) δ (ppm): 161.8 (C-4), 159.2 (C-2), 157.4 (C-2"), 153.9 (C-3"), 151.2 (C-4'), 145.4 (C-9), 130.3 (C-5), 129.1 (C-7), 128.4 (C-2'), 127.8 (C-1'), 117.4 (C-1"), 115.0 (C-5"), 114.3 (C-4"), 113.9 (C-3'), 111.5 (C-6"), 110.5 (C-10), 109.4 (C-6), 55.8 (C-8"), 55.5 (C-7"), 55.4 (C-5'), 30.0 (C-1), 28.3 (C-3); GCMS (EI) calculated for $C_{24}H_{23}N_3O_5$, 433.46 $[M]^+$; observed: 433.20.

5-(2,5-dimethoxyphenyl)-7-(4-methoxyphenyl)-1,3-dimethylpyrido[2,3-*d*]pyrimidine-2,4(1 H,3 H)-dione 2 (l)

Yield: 81%; yellowish brown; m.p.: 172–174 °C; IR (cm^{-1}) ν_{max}: 2941 (C-$H_{aliph.}$), 2360 (C=C), 1692 (C=O); ^{1}H NMR (600 MHz, $CDCl_3$) δ (ppm): 8.04 (d, J=2.0 Hz, 2H, H-2', H-3'), 7.94 (d, J=8.9 Hz, 2 H, H-4', H-5'), 7.22 (s, 1H, H-6), 6.80 (s, 1H, H-3"), 6.75 (d, J=8.4 Hz, 1H, H-5"), 6.58 (d, J=2.3 Hz, 1H, H-6"), 3.86 (s, 3 H, H-7'), 3.79 (s, 3 H, H-7"), 3.73 (s, 3 H, H-8"), 3.38 (s, 3 H, H-1), 2.62 (s, 3 H, H-3); ^{13}C NMR (150 MHz, $CDCl_3$) δ (ppm): 160.4 (C-4), 157.5 (C-2), 155.8 (C-4'), 150.7 (C-4"), 145.3 (C-2"), 132.1 (C-9), 130.6 (C-5), 130.2 (C-7), 129.0 (C-1'), 128.3 (C-2'), 127.9 (C-1"), 121.6 (C-3"), 117.9 (C-5"), 114.0 (C-6"), 113.8 (C-3'), 110.9 (C-10), 109.8 (C-6), 55.6 (C-8"), 55.5 (C-7"), 55.3 (C-5'), 30.0 (C-1), 28.2 (C-3); GCMS (EI) calculated for $C_{24}H_{23}N_3O_5$, 433.46 $[M]^+$; observed: 433.20.

5,7-bis(4-methoxyphenyl)-1,3-dimethylpyrido[2,3-*d*]pyrimidine-2,4(1 H,3 H)-dione 2 (m)

Yield: 79%; brown; m.p.: 162–164 °C; IR (cm^{-1}) ν_{max}: 2942 (C-$H_{aliph.}$), 2360 (C=C), 1697 (C=O); ^{1}H NMR (600 MHz, $CDCl_3$) δ (ppm): 8.11 (d, J=8.8 Hz, 2H, H-2', H-3'), 8.04 (d, J=8.8 Hz, 2 H, H-2", H-3"), 7.44–7.41 (m, 1H, H-4'), 7.40 (s, 1H, H-6), 7.39–7.37 (m, 1H, H-5'), 7.28 (dd, J=7.4, 1.6 Hz, 1H, H-4"), 7.17 (dd, J=7.3, 1.5 Hz, 1H, H-5"), 3.88 (s, 3 H, H-7'), 3.73 (s, 3 H, H-7"), 3.11 (s, 3 H, H-1), 2.58 (s, 3 H, H-3); ^{13}C NMR (150 MHz, $CDCl_3$) δ (ppm): 160.6 (C-4), 159.1 (C-2), 157.5 (C-6'), 155.9 (C-6"), 151.6 (C-9), 145.6 (C-5), 132.1 (C-1"), 130.0 (C-1'), 129.7 (C-7), 129.1 (C-2'), 121.3 (C-2"), 120.5 (C-3"), 117.6 (C-4"), 114.3 (C-3'), 111.0 (C-5"), 110.5 (C-10), 109.6 (C-6), 55.7 (C-5'), 55.4 (C-7"), 30.0 (C-1), 28.3 (C-3); GCMS (EI) calculated for $C_{23}H_{21}N_3O_4$, 403.43 $[M]^+$; observed: 404.10 [M+1].

7-(4-methoxyphenyl)-1,3-dimethyl-5-(naphthalen-2-yl)pyrido[2,3-*d*]pyrimidine-2,4(1 H,3 H)-dione 2 (n)

Yield: 88%; yellowish brown; m.p.: 181–183 °C; IR (cm^{-1}) ν_{max}: 2928 (C-$H_{aliph.}$), 2360 (C=C), 1653 (C=O); ^{1}H NMR (600 MHz, $CDCl_3$) δ (ppm): 8.14 (d, J=8.9 Hz, 1H, H-8"), 8.09 (d, J=8.9 Hz, 2 H, H-2', H-3'), 8.00 (d, J=9.0 Hz, 1H, H-5"), 7.97 (s, 1H, H-6), 7.46 (dd, J=8.4, 1.7 Hz, 1H, H-6"), 7.13 (d, J=8.8 Hz, 1H, H-7"), 7.02 (d, J=8.9 Hz, 2 H, H-3", H-4"), 6.98 (d, J=8.9 Hz, 2 H, H-4', H-5'), 6.93 (s,, 1H, H-1"), 3.86 (s, 3 H, H-7'), 3.15 (s, 3 H, H-1), 2.51 (s, 3 H, H-3); ^{13}C NMR (150 MHz, $CDCl_3$) δ (ppm): 160.7 (C-4), 157.7 (C-2), 156.2 (C-4'), 148.9 (C-9), 137.4 (C-5), 131.9 (C-1'), 130.5 (C-2"), 129.2 (C-3"), 128.4 (C-7), 128.3 (C-2'), 127.9 (C-1"), 127.8 (C-9"), 127.1 (C-10"), 126.8 (C-8"), 126.4 (C-7"), 126.2 (C-6"), 125.1 (C-4"), 117.9 (C-5"), 114.4 (C-10), 113.9 (C-3'), 109.0(C-6), 55.5 (C-5'), 30.2 (C-1), 28.4 (C-3); GCMS (EI) calculated for $C_{26}H_{21}N_3O_3$, 423.15 $[M]^+$; observed: 422.10 [M-1].

Biology

Cell culture and maintenance

Human colorectal cancer (HCT-116), breast cancer (MCF-7), prostate cancer (PC-3), and liver cancer (HepG2) cells were grown in DMEM media containing 10% Fetal Bovine Serum (FBS) and 1% penicillin and streptomycin. It was maintained at 37 °C in an incubator, humidified with 5% CO_2. At 70–80% confluency, the culture cells were trypsinized with 0.25% trypsin-EDTA (Invitrogen) and subcultured for further experimentation [12].

MTT assay

MTT reagent was used in the cytotoxicity assay to test the drug's sensitivity to the cancer cells (HCT-116, MCF-7, PC-3, and HepG2). The reduction of yellow-colored MTT (3-(4,5-Dimethylthiazol-2-yl)-2,5-Diphenyltetrazolium Bromide) into insoluble, dark purple-colored formazan crystals served as the basis for this assay. The cells were seeded in 96-well plates (1×10^4 cells/well) and kept at 37 °C in an incubator with CO_2 filtration for the entire night. They were then treated for 24 to 48 h with varying concentrations (1–50 µM) of synthesized compounds and raltitrexed.

Following the treatments, treated cells were incubated for 4 h at a final concentration of 0.5 mg/ml of MTT. After the incubation period, each well received 200 µL of acidified DMSO to dissolve the purple formazan crystals. The cell culture medium was then carefully aspirated. After putting the plates on a shaker for ten to twenty minutes at room temperature, a microplate reader was used to measure the absorbance at 570 nm. Untreated cells were employed as a control. Raltitrexed was employed as a positive control. Three measurements of each were made. The results were displayed as mean±SEM [13, 14].

Thymidylate synthase inhibitory assay

According to the procedure described by Wahba et al. [15] and Davisson et al. [16], an enzymatic assay for thymidylate synthase was performed. The hTS enzyme was procured from Elabscience using the catalog. No PKSH033115. Thymidylate synthase was assayed spectrophotometrically at 30 °C and pH 7.4 in a mixture

containing 0.1 M 2-mercaptoethanol, 0.0003 M (6*R*, *S*)-tetrahydrofolate, 0.012 M formaldehyde, 0.02 M $MgCl_2$, 0.001 M dUMP, 0.04 M Tris–HCl, and 0.00075 M NaEDTA. The reaction was initiated by the addition of 30 nM hTS, yielding a change in absorbance at 340 nm of 0.019/min in the absence of inhibitor. Inhibitory concentration was then calculated using two inhibitor concentrations (1n, 2j) [17]. The test compounds' concentration–inhibition response curve was then created to ascertain the median inhibitory concentration (IC_{50}). The acquired information was compared with raltitrexed.

In silico study

Molecular docking

Molecular docking study was conducted using the Mac operating system on an Apple I Mac operating Maestro 12.9 (Schrodinger 2022-23) [18]. Using PDB ID: 1HVY (resolution: 1.90 Å), *in silico* studies were carried out to ascertain the binding interaction of the potent compounds within the target protein's active site. The main steps in molecular docking studies are protein preparation and selection, grid creation [19], ligand preparation [20], docking [21], along with subsequent docking analysis [22]. Impurities and other software-reported flaws were eliminated in order to optimize and minimize the protein. The minimized protein was utilized in grid generation, where the chosen ligand served as the reference and represented the drug's binding sites in relation to the target. The LigPrep module developed compounds that were depicted in three dimensions [23]. For every input structure, the molecules were exposed to an OPLS-2005 force field, which produced a single, low-energy 3D structure. Glide software was used to conduct docking studies [24]. It was completed with extra precision and involved XP descriptor data. After that, energy-minimized poses were scored in order to produce a Glide score and docking score. Further, the validation of the docking study was done by using raltitrexed (Fig. 2) [25, 26].

Physicochemical, biochemical, structural, and toxicological (ADME/T) studies

The Schrodinger suite's QikProp module provides a quick and easy way to estimate ligand absorption, distribution, metabolism, and excretion properties. The ADME properties were measured using prepared ligands. It accurately predicts the properties of molecules that are relevant to pharmaceuticals. Prepared molecules were imported from the file for the analysis, and the job was instructed to be executed. The pharmacokinetic characteristics of ligands, including their molecular weight, acceptor and donor hydrogen bonds, QPlogP(o/w), QPlogHERG, QPPMDCK, QPPCaco, QPlogBB, QPlogKp, Polar Surface Area (PSA), and percentage of oral absorption by humans, have been assessed. The application of Lipinski's rule aids in the prediction of the fundamental idea and physiological characteristics of inhibitors [7, 27].

Results and discussion

As depicted in scheme 1, 28 new diaryl-based pyrido[2,3-*d*]pyrimidine/alkyl-substituted pyrido[2,3-*d*]pyrimidine derivatives have been synthesized. Diaryl-based pyrido[2,3-*d*]pyrimidine/alkyl-substituted pyrido[2,3-*d*] pyrimidine derivatives were produced by condensing different substituted acetophenones and substituted benzaldehydes using NaOH as a base, were reacted with 6-aminouracil (I) to obtain diaryl based pyrido[2,3-*d*] pyrimidine derivatives 1(a-n) and then subjected to alkylation with methyl iodide to afford alkylated diaryl pyrido[2,3-*d*]pyrimidine derivatives 2(a-n). Synthesized target compounds were characterized using proton and carbon NMR, GCMS (EI), and melting point characteristics and purified using column chromatography. The purity of potent compounds was further verified by HPLC, results of which revealed that both compounds 1n and 2j had purity of more than 98% (SI). Alkylation of methyl at NH of pyrido[2,3-*d*]pyrimidine can be confirmed by two methyl singlet at 2 to 3.6 ppm in ^{1}H NMR and 20 to 32 ppm in ^{13}C NMR. Further, both carbonyls of alkyl-substituted pyrido[2,3-*d*]pyrimidine were detected between 156 and 175 ppm in ^{13}C NMR.

Biological assessment

In vitro cytotoxicity activity

All the synthesized compounds were assessed for their anticancer properties against four different human cancer cell lines, including HCT 116 (colorectal cancer), MCF-7 (breast cancer), Hep G2 (liver cancer), and PC-3 (prostate cancer). Among all the synthesized compounds, compounds 1n and 2j exhibited excellent anticancer activity against all cancer cell line with IC_{50} values

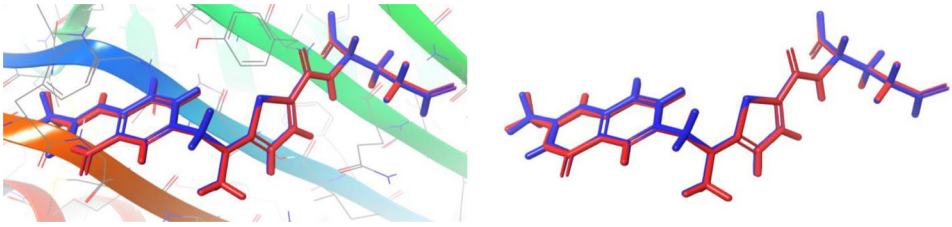

Fig. 2 Overlay of experimental (red) and docked (blue) structures of raltitrexed inside catalytic pocket of human thymidylate synthase (PDB code IHVY)

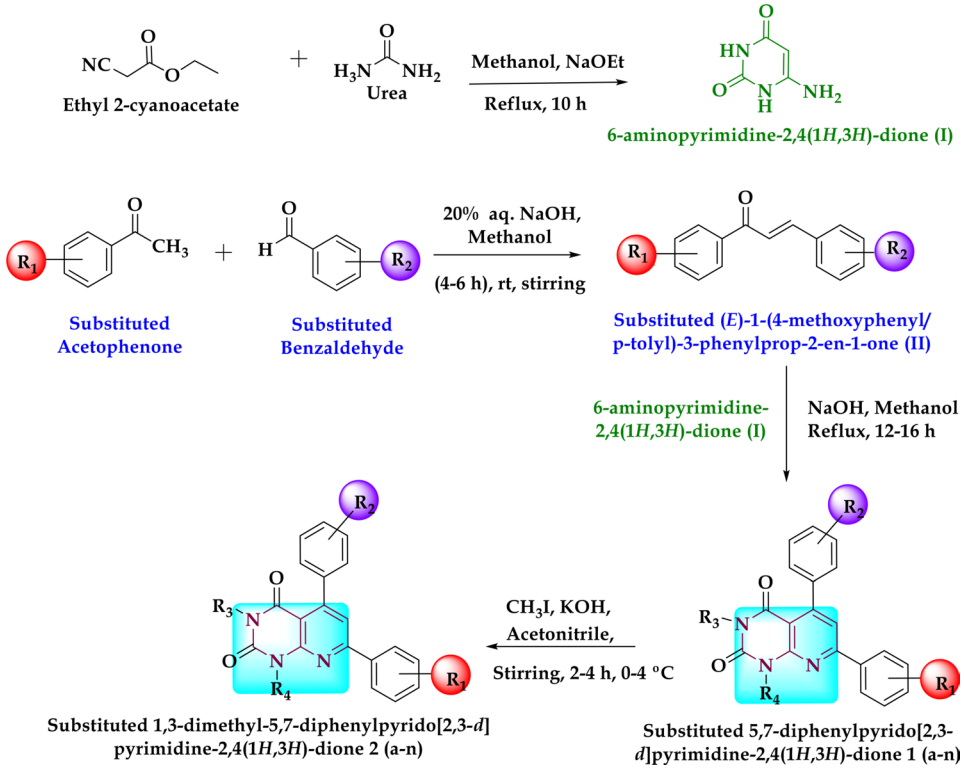

Scheme 1 Synthesis of diaryl based pyrido[2,3-*d*]pyrimidine/ alkyl substituted pyrido[2,3-*d*]pyrimidine derivatives 1 & 2 (a-n)

1.98±0.69, 2.18±0.93, 4.04±1.06, and 4.18±1.87 µM; and 1.48±0.86, 3.18±0.79, 3.44±1.51, and 5.18±1.85 µM, respectively with control raltitrexed (IC_{50} 1.07±1.08, 1.98±0.72, 1.34±1.0 and 3.09±0.96 µM respectively). Compound 1i and 2e also exhibited potent activity at IC_{50} values of 2.98±0.87, 3.59±0.59, 3.81±1.86, and 5.24±1.18 µM; and 4.89±0.09, 6.41±0.84, 7.49±0.87, 9.89±1.64 µM, respectively against respective cell lines. Compound 1a showed good activity against HCT 116, MCF-7, and Hep G2 but more than 10 µM against PC-3 cells. Surprisingly, compound 2k showed very potent activity against HCT 116 (IC_{50} 5.44±1.18 µM), but it was less potent against other cell lines. Further, compound 2n showed potent inhibitory activity against HCT 116 (IC_{50} 5.59±0.93 µM) and MCF-7 (IC_{50} 8.45±1.06 µM) but less potent to Hep G2 and PC-3 cells. Four compounds (1i, 1n, 2e, and 2j) had IC_{50} values lower than 5 µM against HCT 116, and three compounds (1i, 1n, and 2j) against MCF-7 and Hep G2 and 1n against PC-3. Compounds 1a, 1c, 1f, 1 h, 1 m, 2a, 2f, 2i, 2k, and 2n were having IC_{50} values between 5 and 10 µM against HCT 116; compounds 1a, 1 h, 1 m, 2a, 2e and 2n against MCF-7; compounds 1a, 1 m, 2a, 2e, and 2 h against Hep G2; and compounds 1i, 2e, 2 g, 2 h and 2j against PC-3 (Table 2).

From the anticancer results, a structure-activity relationship relationship of synthesized compounds against tested cell lines was depicted as follows:

a. Pyrido[2,3-*d*]pyrimidine pharmacophore was essential for anticancer activity, which is in accordance with the findings of Kumar *et al.*, 2023 [1].
b. Compounds **1n** and **2j** with electron-donating groups at position R and R_1 showed potent activity against all tested cell lines along with excellent TS inhibitory activity with reference to raltitrexed, which is in accordance with the findings of Malagu *et al.*, 2009 [28].
c. Further, compound 2e with methyl groups at N-positions also had potent activity against all tested cell lines. These results are in accordance with the findings of Connolly *et al.*, 1997 and Kumar *et al.*, 2023 [1, 29].
d. Compounds substituted at the para position had the good IC_{50} than those at ortho and meta-positions [30].
e. Compounds 1a, 1f, 1i, 2a, and 2e with electron withdrawing group showed promising activity against HCT 116 and MCF 7 cell lines concerning raltitrexed.
f. Overall, compounds with methyl group at the N-position of pyrido[2,3-*d*]pyrimidine derivatives (2 a-n) had potent activity over compounds having NH (Fig. 3).

Table 2 Antiproliferative activity of synthesized compounds 1 & 2 (a-n)

Cmp.	R_1	R_2	R_3	R_4	HCT 116 (Colorectal cancer)	MCF-7 (Breast cancer)	Hep G2 (Liver cancer)	PC-3 (Prostate cancer)
IC_{50} μM ± SEM[a, b]								
1a	4-CH_3	4-Chloro	H	H	5.44 ± 0.81	9.67 ± 0.62	8.46 ± 1.87	13.57 ± 1.02
1b	4-CH_3	3-F,4-Cl	H	H	11.21 ± 1.80	14.56 ± 1.31	15.68 ± 0.81	21.23 ± 1.41
1c	4-CH_3	4-dimethylamino	H	H	7.66 ± 0.70	10.11 ± 1.81	12.11 ± 1.21	17.45 ± 1.08
1d	4-CH_3	3,4-dimethoxy	H	H	18.99 ± 1.21	26.58 ± 0.95	34.66 ± 1.01	39.11 ± 0.87
1e	4-CH_3	2,6-dichloro	H	H	27.98 ± 1.33	38.97 ± 1.21	42.66 ± 1.67	48.87 ± 1.91
1f	4-OCH_3	3-bromo	H	H	9.77 ± 1.68	13.68 ± 0.69	16.21 ± 0.91	18.47 ± 1.63
1 g	4-OCH_3	2-Chloro	H	H	13.44 ± 0.41	17.46 ± 1.38	18.95 ± 0.67	28.43 ± 0.78
1 h	4-OCH_3	4-bromo	H	H	7.88 ± 0.78	9.94 ± 1.41	11.25 ± 0.73	15.93 ± 1.11
1i	4-OCH_3	4-Chloro	H	H	2.98 ± 0.87	3.59 ± 0.59	3.81 ± 1.86	5.24 ± 1.18
1j	4-OCH_3	4-dimethylamino	H	H	13.69 ± 1.09	21.41 ± 1.07	19.32 ± 1.11	35.84 ± 0.74
1k	4-OCH_3	2,6-dimethoxy	H	H	28.98 ± 1.61	32.32 ± 0.92	36.49 ± 1.42	41.54 ± 1.97
1 L	4-OCH_3	2,5-dimethoxy	H	H	11.75 ± 0.99	14.34 ± 1.91	13.11 ± 0.53	19.11 ± 1.29
1 m	4-OCH_3	4-methoxy	H	H	6.59 ± 0.81	8.38 ± 1.37	9.62 ± 1.87	12.31 ± 1.38
1n	4-OCH_3	4-(naphthalen-2-yl	H	H	**1.98 ± 0.69**	**2.18 ± 0.93**	**4.04 ± 1.06**	**4.18 ± 1.87**
2a	4-CH_3	4-Chloro	CH_3	CH_3	5.87 ± 1.37	7.49 ± 1.83	7.42 ± 0.61	11.67 ± 1.01
2b	4-CH_3	3-F,4-Cl	CH_3	CH_3	21.35 ± 1.50	36.97 ± 1.01	38.78 ± 1.13	41.47 ± 1.85
2c	4-CH_3	4-dimethylamino	CH_3	CH_3	11.99 ± 0.73	15.76 ± 1.49	14.38 ± 0.71	21.52 ± 1.11
2d	4-CH_3	3,4-dimethoxy	CH_3	CH_3	20.78 ± 1.14	29.47 ± 0.76	32.46 ± 1.61	38.87 ± 1.72
2e	4-CH_3	2,6-dichloro	CH_3	CH_3	4.89 ± 0.09	6.41 ± 0.84	7.49 ± 0.87	9.89 ± 1.64
2f	4-OCH_3	3-bromo	CH_3	CH_3	7.88 ± 0.88	13.47 ± 1.19	12.38 ± 1.51	18.37 ± 0.97
2 g	4-OCH_3	2-Chloro	CH_3	CH_3	14.11 ± 1.80	21.48 ± 1.63	18.93 ± 1.88	6.79 ± 1.71
2 h	4-OCH_3	4-bromo	CH_3	CH_3	10.77 ± 0.79	29.37 ± 0.95	8.49 ± 1.09	8.58 ± 1.41
2i	4-OCH_3	4-Chloro	CH_3	CH_3	7.54 ± 1.11	14.38 ± 1.72	17.26 ± 1.15	13.52 ± 1.21
2j	4-OCH_3	4-dimethylamino	CH_3	CH_3	**1.48 ± 0.86**	**3.18 ± 0.79**	**3.44 ± 1.51**	**5.18 ± 1.85**
2k	4-OCH_3	2,6-dimethoxy	CH_3	CH_3	5.44 ± 1.18	11.31 ± 1.91	10.47 ± 0.86	18.58 ± 1.06
2 L	4-OCH_3	2,5-dimethoxy	CH_3	CH_3	11.11 ± 0.71	19.84 ± 1.33	16.38 ± 1.09	24.55 ± 1.91
2 m	4-OCH_3	4-methoxy	CH_3	CH_3	11.57 ± 1.26	18.57 ± 1.82	17.31 ± 1.71	26.23 ± 1.43
2n	4-OCH_3	4-(naphthalen-2-yl	CH_3	CH_3	5.59 ± 0.93	8.45 ± 1.06	11.39 ± 0.94	12.49 ± 1.04
Raltitrexed					1.07 ± 1.08	1.98 ± 0.72	1.34 ± 1.01	3.09 ± 0.96

a- The assay was performed in triplicate, and data were compiled for 48 h incubation; b- Data were presented as means ± standard error mean of three independent experiments

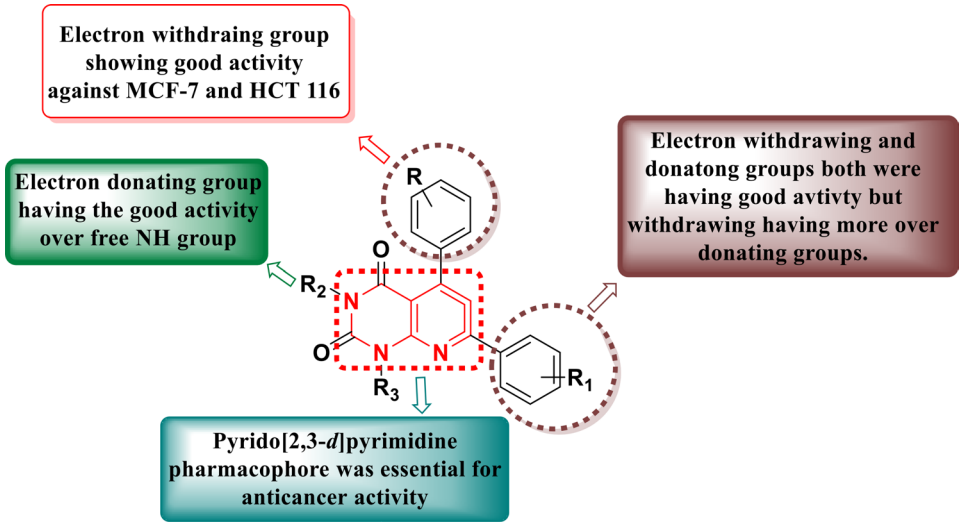

Fig. 3 Structure-activity relationship based on anticancer activity of synthesized compounds 1 &2 (a-n)

Table 3 In vitro thymidylate synthase (TS) activity of compounds 1n and 2j, along with raltitrexed

Compound No.	IC_{50} (nM) ± SEM[a, b]
1n	20.47 ± 1.09
2j	13.48 ± 0.96
Raltitrexed	14.95 ± 1.01

a- Assay was performed in triplicate; b- Data were presented as means ± standard error mean of three independent experiments

In vitro thymidylate synthase (TS) inhibitory activity

The most potent compounds in the cytotoxic assay (1n and 2j) were further examined to ascertain their inhibitory effects against thymidylate synthase (TS) with the objective of identifying these molecules' likely mechanism of action as anticancer medications. Raltitrexed was used as control for this activity and the results were reported as IC_{50} (Table 3). With IC_{50} concentrations of 20.47 ± 1.09 and 13.48 ± 0.96 nM, the tested compounds 1n and 2j demonstrated good inhibitory activity that was in line with their proven in vitro anticancer effects with control raltitrexed (IC_{50} 14.95 ± 1.01 nM).

Evaluation of *insilico* study

Molecular docking analysis

Hydrophobic interactions and hydrogen bonds, which are generally highlighted by protein-ligand interactions, are essential to predict the binding conformation of ligands with hTS. The binding conformations of synthesized compounds in the binding pocket of thymidylate synthase have been analyzed.

To explore the possible binding mechanisms of compounds at the catalytic site, flexible docking of compounds with raltitrexed into the hTS active site (PDB: IHVY) was done with the aid of Glide in Schrödinger. The catalytic gatekeeper residue cys195 has been associated to the pyridogrido[2,3-*d*]pyrimidine core. Previous research [7], has shown that interactions occur frequently and that cysteine sulfur is often found in the same plane as the fundamental ring system (Fig. 4). The docked ligands 1n and 2j exhibited polar interactions with Gln, Ser, Thr, Asn, and Asn; hydrophobic interactions with Phe, Tyr, Ala, Met Ile, Trp, Leu, Ile, and Cys; and charged interactions with Arg, Glu and Asp amino acid residue (Table 4). When compared to raltitrexed, the potent compounds 1n and 2j displayed superior docking scores.

Analysis of physicochemical, biochemical, structural, and toxicological characteristics (ADME/T) of compounds 1n and 2j

The ADME/T parameters for the compounds 1n and 2j with good activity have been determined. ADME is a crucial pharmacological measure to assess the bioavailability, absorption, and other pharmacokinetic characteristics of potent compounds 1n and 2j. It was found that the pharmacokinetic properties of the potent compounds against the thymidylate synthase were within the acceptable range (Table 5).

Molecular weight was expressed as MW, and partition coefficient QPlogP (o/w) ranged from −2 to 6.5, and the predicted brain/blood partition coefficient (QPlogBB) was within the accepted range of -3.0 to -1.2. The predicted skin permeability range (QPlogKp) spans from −8 to -1. For apparent gut-blood barrier permeability (QPP Caco), values ≤ 25 suggest poor permeability, while values ≥ 500 indicate high permeability. The forecast for human serum albumin binding (QPlogKhsa) ranges from −1.5 to 1.2. Moreover, the percent of human oral absorption (HA) is categorized as high if ≥ 80% and low if ≤ 25%. Donor HB: The anticipated count of hydrogen bond donors should not exceed 5. Acceptor HB: The projected number of hydrogen bond acceptors should remain below 10. Polar Surface Area (PSA) falls within the range of < 90 Å, indicating favorable, and > 140 Å, suggesting unfavorable. QPlogHERG: Predicted IC_{50} value for blockage of HERG K^+ channels ≤ -5 good; QPPMDCK: Predicted apparent MDCK cell permeability accepted range ≤ 25 poor, ≥ 500 excellent.

Conclusion

In the present study, we designed and synthesized 28 new diaryl-based pyrido[2,3-*d*]pyrimidine/alkyl-substituted pyrido[2,3-*d*]pyrimidine derivatives as anticancer agents against colorectal, breast, liver, and prostate cancer cell lines with positive control raltitrexed. Tested compounds 1j and 2n demonstrated strong TS inhibitory activity with IC_{50} of 20.47 ± 1.09 and 13.48 ± 0.96 nM with control raltitrexed (IC_{50} 14.95 nM). Compounds 1j and 2n showed potent anticancer activity with IC_{50} values of 1.98 ± 0.69, 2.18 ± 0.93, 4.04 ± 1.06, and 4.18 ± 1.87 μM; and 1.48 ± 0.86,3.18 ± 0.79, 3.44 ± 1.51, and 5.18 ± 1.85 μM, respectively with control raltitrexed (IC_{50} 1.07 ± 1.08, 1.98 ± 0.72, 1.34 ± 1.0, and 3.09 ± 0.96 μM, respectively). Potent compounds 1j and 2n showed good docking scores of -10.6 and −9.5 kcal/mol, respectively with reference raltitrexed (-9.4 kcal/mol), and are having polar interactions with Gln, Ser, Thr, Asn, and Asn; hydrophobic interactions with Phe, Tyr, Ala, Met Ile, Trp, Leu, Ile, and Cys; and charged interactions with Arg, Glu and Asp amino acid residue with catalytic amino acid Cys195. Further, synthesized compounds 1j and 2n satisfied Lipinski criteria, suggesting good drug-like qualities with good oral bioavailability profile. Based on the aforementioned results, compounds 1j and 2n may be developed as promising inhibitors of TS.

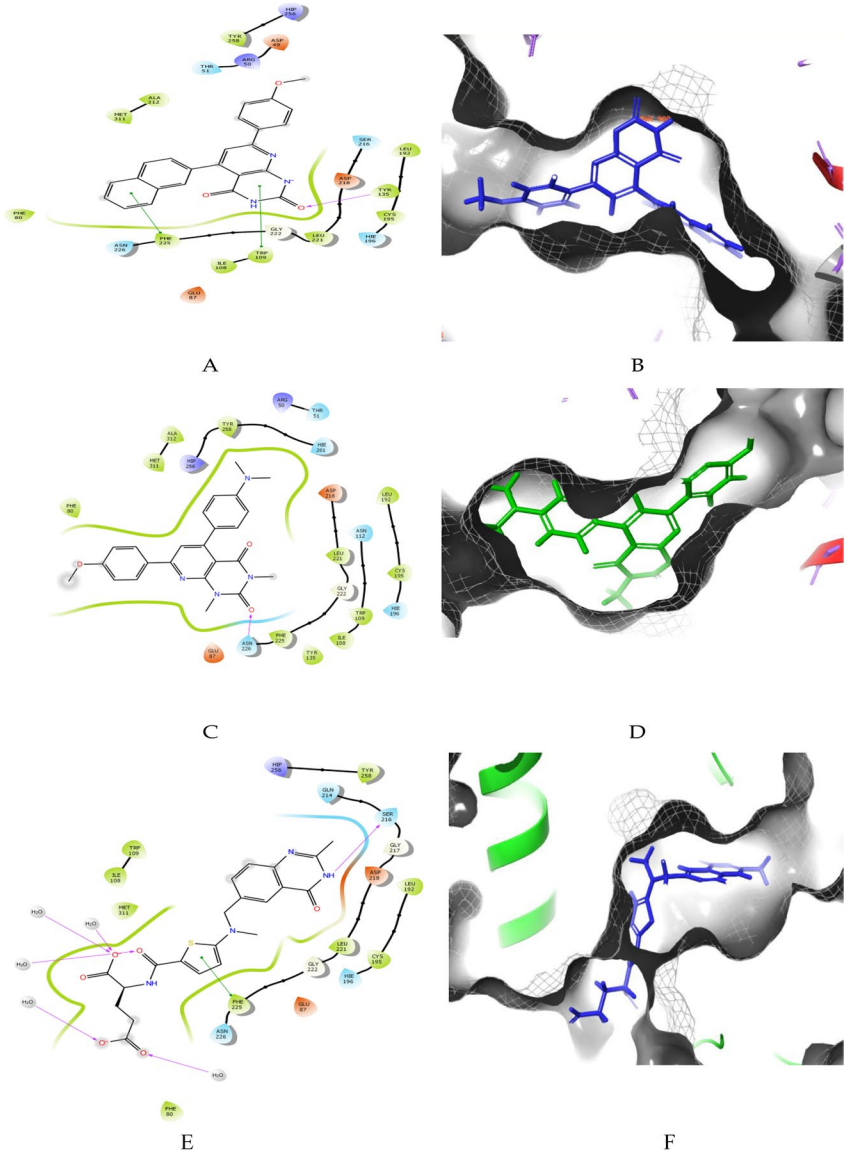

Fig. 4 **A**, **C**, and **E** were 2D docking orientations of compounds 1n, 2j, and raltitrexed, respectively, in the active site of hTS, demonstrating binding and significant interactions with some of the key amino acid residues; **B** and **D** were the orientations of the diaryl based pyrido[2,3-*d*]pyrimidine core in a close-up view of compounds 1n and 2j; **F** was the close-up view of raltitrexed inside catalytic pocket of hTS (PDB code IHVY)

Table 4 Interaction pattern of compounds 1n, and 2j along with raltitrexed

S. No.	Cpd.	H-Bonding	Hydrophobic	Polar	Charged	Pi-cation	Docking Score (Kcal/mol)
1	1n	Tyr135	Phe80, Ile108, Trp109, Tyr135, Leu192, Cys195, Leu221, Phe225, Tyr258, Met311, and Ala312	Thr51, Hie196, Ser216, and Asn226	Asp49, Arg50,Glu87,Asp218, Hip256,	Asp49,Arg50, Glu87,	-10.6
2	2j	Asn226	Phe80, Ile108, Trp109, Tyr135, Leu192, Cys195, Leu221, Phe225, Tyr258, Met311, and Ala312	Thr51, Asn112, Hie196, Ser216, Asn226 and Hie261	Glu87, Arg50, Glu87, Asp218 and Hip256,	Glu87, Asp218	-9.5
3	Ral	Ser216	Phe80, Ile108, Trp109, Leu192, Cys195, Leu221, Phe225, Tyr258, and Met311	Hie196, Gln214, Ser216, and Asn226	Glu87, Asp218, Hip256	Glu87, Asp218	-9.4

Table 5 Physicochemical, biochemical, structural, and toxicological characteristics (ADME/T) of compounds 1n and 2j

S. No	Compound	MW	Donor HB	Acceptor HB	QPlogP o/w	QPP Caco	QPlogBB	QPlogK hsa	QPlogKp	PSA	QPlogHERG	QPPMDCK	%HA
1	1n	395.12	2	4.86	3.82	309.1	-0.78	0.623	-2.38	100.7	-8.6	197.150	96
2	2j	416.18	0	4.76	4.67	369.6	-1.12	0.467	-1.41	80.3	-8.2	208.194	100
3	Raltitrexed	458.48	3	9.25	2.4	0.321	-3.62	0.347	-6.51	190.1	-2.6	0.173	36

Abbreviations

CRC	Colorectal cancer
hTS	Human thymidylate synthase
TS	Thymidylate synthase
Ral	Raltitrexed
IC_{50}	Concentration which inhibits 50% of the tested population
nM	Nano molar
μM	Micro molar
THF	Tetrahydrofolate
dUMP	deoxyUridine monophosphate
dTMP	deoxyThymidine monophosphate
Aq	Aqueous
Eq	Equivalent
GCMS	Gas Chromatography-mass spectrometry

Supplementary Information

The online version contains supplementary material available at https://doi.org/10.1186/s13065-024-01228-w.

Supplementary Material 1

Acknowledgements
The authors are thankful to the CIL-Central University of Punjab and DST-FIST for providing Infrastructural support for the completion of this study. The authors are also thankful to DST SERB (CRG/2023/001580) for financial support.

Author contributions
Adarsh Kumar, Nabeel Backer, and Harshali Paliwal synthesized the molecules, Ankit Kumar Singh and Tanushree Debbaraman performed anticancer activity, Vikramjeet Singh and Adarsh Kumar performed molecular docking studies, Pradeep Kumar and Adarsh Kumar wrote the manuscript.

Funding
There was no specific funding for this research.

Data availability
Data is provided within the manuscript or supplementary information files.

Declarations

Ethics approval and consent to participate
Not applicable.

Consent for publication
Not applicable.

Competing interests
The authors declare no competing interests.

Received: 29 February 2024 / Accepted: 13 June 2024
Published online: 28 August 2024

References

1. Kumar A, Bhagat KK, Singh AK, Singh H, Angre T, Verma A, Khalilullah H, Jaremko M, Emwas A-H, Kumar P. Medicinal chemistry perspective of pyrido [2, 3-d] pyrimidines as anticancer agents. RSC Advan. 2023;13(10):6872–908.
2. Deep A, Kumar P, Narasimhan B, Lim SM, Ramasamy K, Mishra RK, Mani V. 2-Azetidinone derivatives. Synthesis, antimicrobial, anticancer evaluation and QSAR studies. Acta Pol Pharm. 2016;73(1):65–78.
3. Saini M, Kumar P, Kumar M, Ramasamy K, Mani V, Mishra RK, Majeed ABA, Narasimhan B. Synthesis, in vitro antimicrobial, anticancer evaluation and QSAR studies of N′-(substituted)-4-(butan-2-lideneamino) benzohydrazides. Arab J Chem. 2014;7(4):448–60.
4. Kumar A, Singh AK, Singh H, Thareja S, Kumar P. Regulation of thymidylate synthase: an approach to overcome 5-FU resistance in colorectal cancer. Med Oncol. 2022;40(1):3.

5. Bray F, Laversanne M, Sung H, Ferlay J, Siegel RL, Soerjomataram I, Jemal A. Global cancer statistics 2022: GLOBOCAN estimates of incidence and mortality worldwide for 36 cancers in 185 countries. Ca-Cancer J Clin. 2024; 1–35.
6. Siegel RL, Miller KD, Goding Sauer A, Fedewa SA, Butterly LF, Anderson JC, Cercek A, Smith RA, Jemal A. Colorectal cancer statistics, 2020. Ca-Cancer J Clin. 2020;70(3):145–64.
7. Kumar A, Novak J, Singh AK, Singh H, Thareja S, Pathak P, Grishina M, Verma A, Kumar P. Virtual screening, structure based pharmacophore mapping, and molecular simulation studies of pyrido [2, 3-d] pyrimidines as selective thymidylate synthase inhibitors. J Biomol Struct Dyn. 2023;41(23):14197–211.
8. Kumar A, Singh AK, Singh H, Vijayan V, Kumar D, Naik J, Thareja S, Yadav JP, Pathak P, Grishina M. Nitrogen Containing Heterocycles as Anticancer agents: a Medicinal Chemistry Perspective. Pharmaceuticals. 2023;16(2):299.
9. Fares M, Abou-Seri SM, Abdel-Aziz HA, Abbas SE-S, Youssef MM, Eladwy RA. Synthesis and antitumor activity of pyrido [2, 3-d] pyrimidine and pyrido [2, 3-d][1, 2, 4] triazolo [4, 3-a] pyrimidine derivatives that induce apoptosis through G1 cell-cycle arrest. Eur J Med Chem. 2014;83:155–66.
10. Barrowcliff M, Carr FH. Organic Medicinal Chemicals (synthetic and Natural): Baillière, Tindall and Cox; 1921; 243–244.
11. Kuday H, Sonmez F, Bilen C, Yavuz E, Gençer N, Kucukislamoglu M. Synthesis and in vitro inhibition effect of new pyrido [2, 3-d] pyrimidine derivatives on erythrocyte carbonic anhydrase I and II. Biomed Res Int. 2014;1–8. https://doi.org/10.1155/2014/594879.
12. Sarkar B, Dhiman M, Mittal S, Mantha AK. Curcumin revitalizes amyloid beta (25–35)-induced and organophosphate pesticides pestered neurotoxicity in SH-SY5Y and IMR-32 cells via activation of APE1 and Nrf2. Metab Brain Dis. 2017;32:2045–61.
13. Kumar M, Joshi G, Arora S, Singh T, Biswas S, Sharma N, Bhat ZR, Tikoo K, Singh S, Kumar R. Design and synthesis of non-covalent imidazo [1, 2-a] quinoxaline-based inhibitors of EGFR and their anti-cancer assessment. Molecules. 2021;26(5):1490.
14. Dhiman M, Zago MP, Nunez S, Amoroso A, Rementeria H, Dousset P, Burgos FN, Garg NJ. Cardiac-oxidized antigens are targets of immune recognition by antibodies and potential molecular determinants in chagas disease pathogenesis. PLoS ONE. 2012;7(1):e28449.
15. Wahba AJ, Friedkin M. The enzymatic synthesis of thymidylate. I. early steps in the purification of thymidylate synthetase of Escherichia coli. J Biol Chem. 1962;237(12):3794–801.
16. Davisson V, Sirawaraporn W, Santi DV. Expression of human thymidylate synthase in Escherichia coli. J Biol Chem. 1989;264(16):9145–8.
17. Amin LH, Shawer TZ, El-Naggar AM, El-Sehrawi HM. Design, synthesis, anticancer evaluation and docking studies of new pyrimidine derivatives as potent thymidylate synthase inhibitors. Bioorg Chem. 2019;91:103159.
18. Kumar R, Kumar A, Singh A, Kumar P. Design, synthesis and molecular Docking studies pyrazoline derivatives as PI3K inhibitors. Comb Chem High Throughput Screen. 2023. https://doi.org/10.2174/1386207326666230504163312.
19. Guleria M, Kumar A, Kumar P. Synthesis and *in silico* studies of quinazolinones as PARP-1 inhibitors. Comb Chem High Throughput Screen. 2023. https://doi.org/10.2174/1386207326666230905153443.
20. Sharma A, Kumar A, Singh AK, Singh H, Kumar KJ, Kumar P. Phytochemical profiling and pharmacological evaluation of Leaf extracts of Ruellia tuberosa L.: an in Vitro and *in silico* Approach. Chem Biodivers. 2023;20(9):e202300495.
21. Shah M, Kumar A, Singh AK, Singh H, Narasimhan B, Kumar P. *In silico* studies of Indole Derivatives as Antibacterial agents. J Pharmacopunct. 2023;26(2):147.
22. Pauly I, Kumar Singh A, Kumar A, Singh Y, Thareja S, Kamal MA, Verma A, Kumar P. Current insights and molecular docking studies of the drugs under clinical trial as RdRp inhibitors in COVID-19 treatment. Curr Pharm Des. 2022;28(46):3677–705.
23. Singh AK, Kumar A, Arora S, Kumar R, Verma A, Khalilullah H, Jaremko M, Emwas AH, Kumar P. Current insights and molecular docking studies of HIV-1 reverse transcriptase inhibitors. Chem Biol Drug Des. 2023;103(1):e14372.
24. Ram T, Singh AK, Pathak P, Kumar A, Singh H, Grishina M, Novak J, Kumar P. Design, one-pot synthesis, computational and biological evaluation of diaryl benzimidazole derivatives as MEK inhibitors. J Biomol Struct Dyn 2023; 1–16.
25. Singh AK, Novak J, Kumar A, Singh H, Thareja S, Pathak P, Grishina M, Verma A, Yadav JP, Khalilullah H. Gaussian field-based 3D-QSAR and molecular simulation studies to design potent pyrimidine–sulfonamide hybrids as selective BRAF V600E inhibitors. RSC Advan. 2022;12(46):30181–200.
26. Kumar A, Singh AK, Thareja S, Kumar P. A review of pyridine and pyrimidine derivatives as Anti-MRSA agents. Anti-Infect Agents. 2023;21(2):18–40.
27. Bisht G, Singh KA, Kumar A, Kumar P. A mechanistic study of the antibacterial activity of phytoconstituents of Pyracantha crenulata by using Molecular Docking studies. Curr Chin Chem 2022; (2): e220722206994.
28. Malagu K, Duggan H, Menear K, Hummersone M, Gomez S, Bailey C, Edwards P, Drzewiecki J, Leroux F, Quesada MJ, Hermann G. The discovery and optimisation of pyrido [2, 3-d] pyrimidine-2, 4-diamines as potent and selective inhibitors of mTOR kinase. Bioorg Med Chem Lett. 2009;19:5950–3.
29. Connolly CJ, Hamby JM, Schroeder MC, Barvian M, Lu GH, Panek RL, Amar A, Shen C, Kraker AJ, Fry DW, Klohs WD. Discovery and structure-activity studies of a novel series of pyrido [2, 3-d] pyrimidine tyrosine kinase inhibitors. Bioorg Med Chem Lett. 1997;7:2415–20.
30. Goldstein DM, Soth M, Gabriel T, Dewdney N, Kuglstatter A, Arzeno H, Chen J, Bingenheimer W, Dalrymple SA, Dunn J, Farrell R. Discovery of 6-(2, 4-Difluorophenoxy)-2-[3-hydroxy-1-(2-hydroxyethyl) propylamino]-8-methyl-8 H-pyrido [2, 3-d] pyrimidin-7-one (Pamapimod) and 6-(2, 4-Difluorophenoxy)-8-methyl-2-(tetrahydro-2 H-pyran-4-ylamino) pyrido [2, 3-d] pyrimidin-7 (8 H)-one (R1487) as orally bioavailable and highly selective inhibitors of p38α mitogen-activated protein kinase. J Med Chem. 2011;54:2255–65.

Publisher's Note